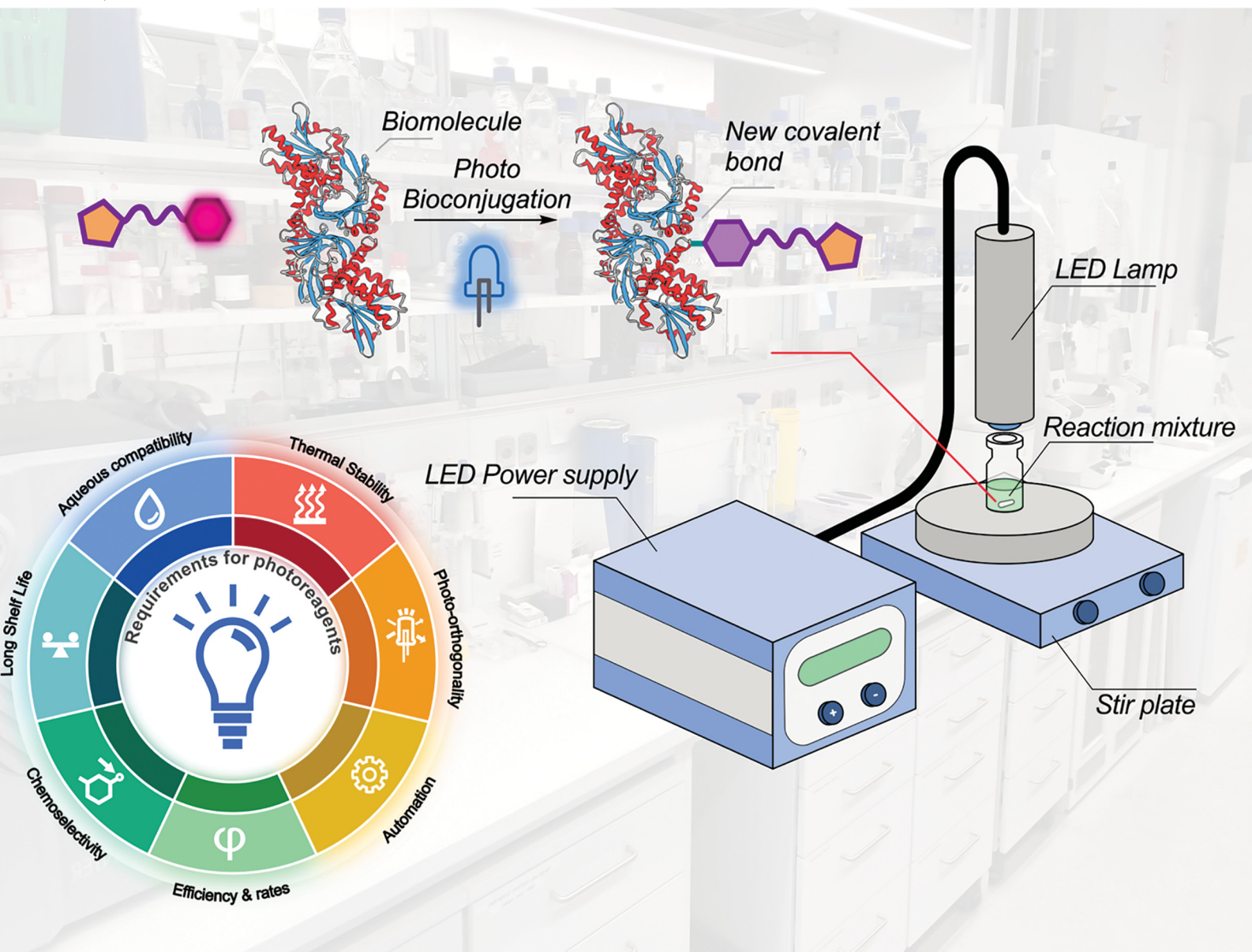


# ChemComm

Chemical Communications

rsc.li/chemcomm



ISSN 1359-7345



Cite this: *Chem. Commun.*, 2025, 61, 5234

## Light-induced chemistry for protein functionalisation

Cesare Berton and Jason P. Holland \*

Derivatising biomolecules like monoclonal antibodies with drugs or imaging agents, whilst preserving their bioactivity, is a challenging task. Protein functionalisation ideally requires methods that operate under mild conditions, are rapid, efficient (high yielding), chemoselective or site-specific, and importantly, non-denaturing. A broad collection of thermally mediated reagents for direct labelling using protein-based reactivity, or bioorthogonal strategies, has been developed, but arguably the most exciting opportunities lie in the application of photochemistry to create new covalent bioconjugate bonds. With current chemical methods for auxochromic tuning of the spectral features of photoactive groups, and with cheap, high-powered light-emitting diodes with precise emission properties, it has never been easier to explore the use of light-induced chemistry for making protein-based bioactive molecules. In biomedicine, the nature of the covalent bond to the protein can have a dramatic impact on the physicochemical properties and performance of the protein-conjugate. Photochemical methods provide access to new types of covalent linkages on protein with the potential to fine-tune biological interactions, leading to improvements in target uptake, binding specificity, metabolic processing, and washout kinetics *in vivo*. This perspective/review highlights recent advances in the development of photoactive reagents for protein labelling. We also discuss the experimental conditions and critical requirements to implement light-induced synthesis of functionalised protein-conjugates in aqueous media effectively.

Received 12th December 2024,  
Accepted 10th March 2025

DOI: 10.1039/d4cc06529h

[rsc.li/chemcomm](http://rsc.li/chemcomm)

## Introduction

The synthesis of functionalised proteins plays a central role in modern biochemical technologies and in new medicines.<sup>1–3</sup> For example, antibody-drug conjugates (ADC), and monoclonal antibodies (or related fragments) labelled with fluorescent tags or radioactive payloads underpin state-of-the-art developments in diagnostic imaging and molecularly targeted (radio)therapies.<sup>4,5</sup> Bioconjugation chemistry – the ability to form new covalent bonds to protein – lies at the core of these technologies.<sup>6–8</sup> Traditional methods for labelling proteins include the use of reagents featuring activated esters like *N*-hydroxysuccinimide (NHS), or benzyl-iso(thio)cyanates (Bn-NCS) that react with the primary  $\epsilon$ -NH<sub>2</sub> side chain of lysine residues.<sup>9</sup> Other common examples include chemoselective derivatisation of free sulphydryl groups on cysteine residues by using reagents that present Michael acceptors like maleimides. Several site-specific enzyme-mediated processes, as well as bioorthogonal reaction pairs, have also been developed to increase control over the chemical composition of the

functionalised protein.<sup>10–12</sup> Others have also explored Ni metal ion<sup>13,14</sup> mediated bioconjugation and protein tagging using Au-complexes.<sup>15</sup> These thermally mediated bioconjugation strategies work well and have led to over 13 clinically validated ADC (and 3 more expected to be approved by FDA in 2025)<sup>16</sup> agents as well as countless examples of fluorescent probes for biochemical analysis in microscopy and related methods, and an increasing number of radiolabelled antibodies for nuclear imaging with positron emission tomography (PET) and radioimmunotherapy (RIT).<sup>17</sup>

When developing new bioconjugation methods to functionalise proteins, a mandatory requirement is to retain the biological integrity of the protein. In practice, this requirement is challenging to fulfil because biomolecules like monoclonal antibodies (mAbs) can be highly sensitive to changes in their physicochemical properties. Fast reaction rates are also ideal for bioconjugate chemistry to ensure efficient and high-yielding reactions when working with protein at low (nano-to-micromolar) concentrations. Many classic bioconjugation methods are relatively slow and incompatible with protein formulation buffers. Employing most classic bioconjugation methods requires pre-processing of the protein sample to alternate conditions that favour the functionalisation step, but this often destabilises the protein leading to denaturation

Department of Chemistry, University of Zurich, Winterthurerstrasse 190, CH-8057 Zurich, Switzerland. E-mail: [jason.holland@chem.uzh.ch](mailto:jason.holland@chem.uzh.ch); Web: <https://www.hollandlab.org>; Tel: +41-44-63-53990



or aggregation. Modern enzymatic methods can address these issues, although they require access to expensive reagents (tailored enzymes with modified active sites that accommodate non-native substrates).<sup>1</sup> Bioorthogonal chemistries are also promising but typically rely on pre-functionalisation of the protein with one of the reaction partners through either protein engineering or enzyme reactions, which is then later labelled in a fast, bioorthogonal step.<sup>18</sup> Since the nature of the bioconjugate bond can dramatically impact the performance of a protein conjugate – through modification of the target specificity and binding, as well as the overall pharmacokinetic profile *in vivo* – new methods for creating bioconjugate bonds are essential.<sup>19–21</sup>

Photochemistry offers several advantages as a means of tagging proteins with bioactive drug molecules or imaging probes.<sup>20,22–25</sup> Benefits include: (i) the initiation of the photo-reaction under ambient conditions through the application of light at wavelengths that do not inflict photodamage on the protein, (ii) rapid reaction rates using highly reactive intermediates generated from the initial photolysis step, (iii) tolerance of the bioconjugation reactions toward complex biological media, particularly components of the protein formulation buffer employed in the stabilisation of clinical-grade monoclonal antibodies, and (iv) the potential to automate the bioconjugation step using advanced flow-based or reactor based machines. Photochemistry also facilitates the synthesis of new types of reactive handles<sup>26,27</sup> or bioconjugate bonds that have yet to be tested *in vivo*. Accessing different covalent bonds to protein can help fine-tune the performance of protein

conjugates with the goals of speeding up the synthesis, improving target uptake, and harnessing new or alternative modes of metabolism to control the pharmacokinetic profile of the agent. Improved chemical control over the adsorption, distribution, metabolism, and excretion (ADME) profile of a protein conjugate can reduce off-target binding alleviating chemotoxicity or radiation dosimetry issues, and thus, improving the therapeutic index of the next generation of drugs. Although highly promising, implementing photochemical methods to derivatise proteins remains challenging because new reagents must be synthesised, and the experimental design is more complex than established conjugation protocols.<sup>28</sup>

The original use of photochemistry for tagging proteins has a rich history that dates back to the concept of photoaffinity labelling (PAL) introduced by Westheimer and co-workers in 1962 (Fig. 1).<sup>29</sup> Subsequent work spanning a timeline up until the 21st Century focused on developing new photoactive handles that can be easily introduced to drug molecules for screening drug-target interactomes.<sup>29–41</sup> The basic idea in PAL is that a pre-equilibrium between a biologically active ligand (e.g. drug molecule) and the target protein is established. Subsequently, irradiation with light of a specific wavelength activates the photoreagent, stimulating the formation of highly reactive intermediates such as carbenes, nitrenes, diradicals, and powerful electrophiles. These intermediates react rapidly with protein-based nucleophiles near the binding site of the PAL reagent. In the process, the covalent bioconjugate bond is formed on a timescale ranging from picoseconds to microseconds (Scheme 1A). This mechanism is extremely useful in



Cesare Berton

photoacids under the guidance of Prof. Cristian Pezzato. From 2023 onwards, he has been part of the group of Prof. Jason Holland as a postdoc, working on the synthesis of novel radiopharmaceuticals by using supramolecular and photochemical methods.



Jason P. Holland

Jason P. Holland is from Yorkshire in the United Kingdom and received a master's degree in Chemistry from the University of York (MChem, 2004) followed by a doctorate from the University of Oxford (DPhil, 2008) with Prof. Jennifer Green and Prof. Jonathan R. Dilworth. He trained as postdoctoral scholar with Prof. Jason S. Lewis in radiochemistry and translational molecular imaging at Memorial Sloan-Kettering Cancer Center in New York (2008–2010). He was then awarded an ETH Fellowship and worked at ETH Zürich and the Paul Scherrer Institute (2010–2012). He was then appointed as Assistant in Chemistry in the Division of Nuclear Medicine and Molecular Imaging at Massachusetts General Hospital, Boston, with a joint faculty appointment as an Instructor in Radiology at Harvard Medical School (2012–2014). In 2015, he worked in the Department of Nuclear Medicine at the University Hospital Freiburg as a Visiting Scientist. In 2022 he was appointed as the Chair of Medicinal Radiochemistry in the Department of Chemistry at the University of Zurich.



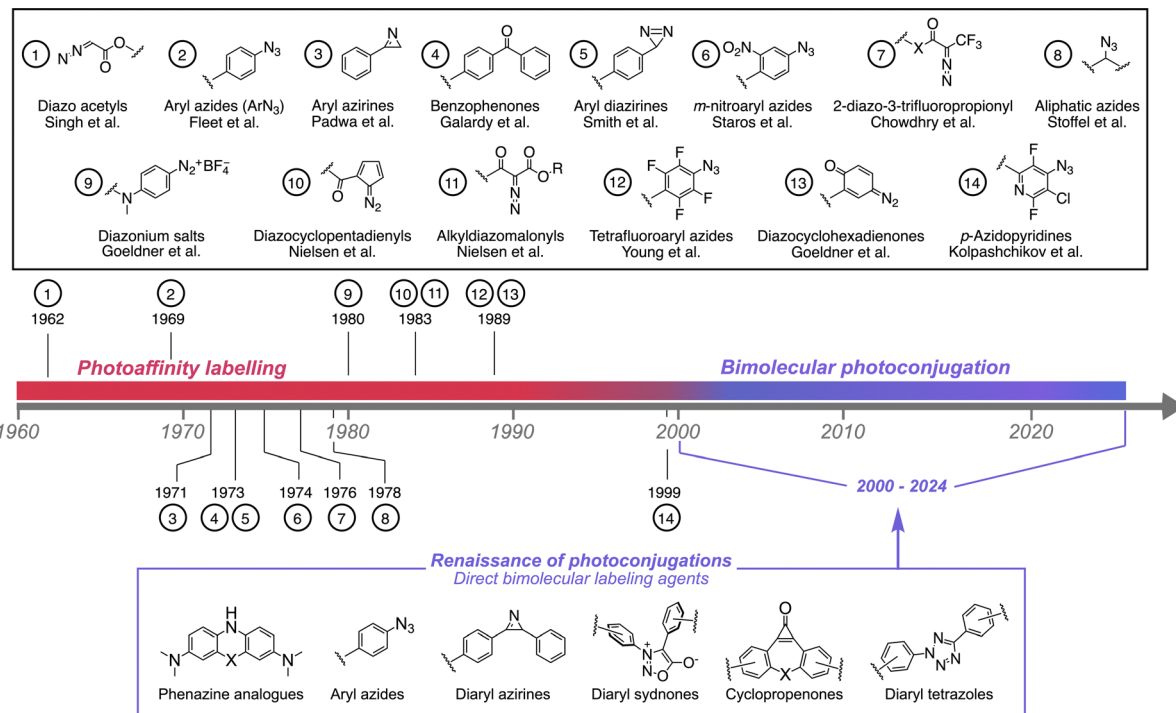
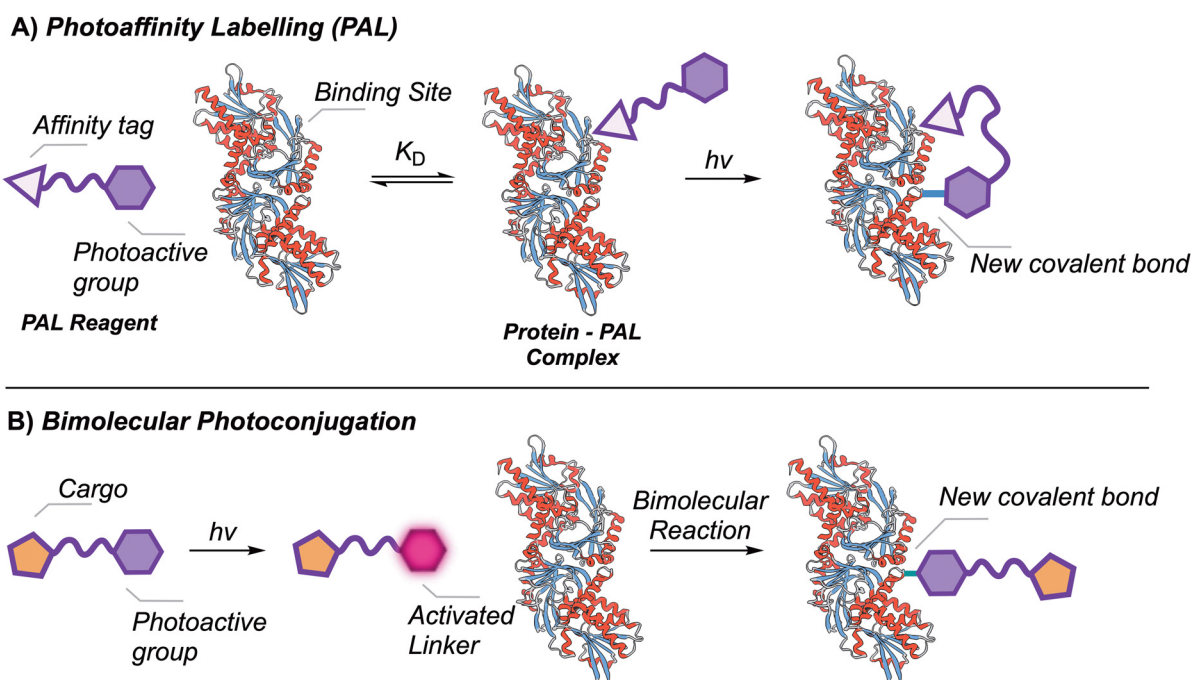


Fig. 1 Timeline of the progression of photoreagents and their applications in biochemistry or medicinal chemistry.



**Scheme 1** Mechanistic differences in the use of light-induced reactions to create covalent bioconjugate bonds on protein via the established concept of (A) photoaffinity labelling with preassociation between the photoreagent and a drug binding site on protein, and (B) direct, bimolecular labelling without preassociation.

characterising the binding profile, the protein selectivity, and the mechanism of action for new drug entities.<sup>42</sup> However, for the light-induced functionalisation of proteins like

immunoglobulins (IgGs) and related fragments, which do not have recognised drug binding sites, a more general bimolecular approach is needed (Scheme 1B).<sup>20,22</sup>

Recent reports on the use of light-induced labelling of bioactive proteins have exploited the photochemistry of many different functional groups such as aryl azides, tetrazoles, azirines, diazirines, benzophenones, and photoredox systems (Fig. 1, blue box). The chemistry of these (and other) photo-reagents is described in the following sections. The photo-induced processes are stratified into three distinct mechanistic classes. In addition, we begin by presenting a set of idealised requirements for developing new photoreagents in the context of labelling bioactive proteins, as well as a discussion of the experimental aspects that must be considered when using photochemistry in synthesis.

## Requirements for light-induced bioconjugation processes

In an ideal photo-induced bioconjugation reaction, several different criteria apply (Fig. 2). First, the reagents should be stable toward thermal degradation, reacting only when exposed to photons of a specific wavelength. Second, to avoid photo-degradation of the protein component, photoactivation of the reagents should occur at wavelengths where the protein of interest does not absorb (photo-orthogonality). Contrary to some assertions which suggest that lower energy photons are optimal, we believe that to prolong the shelf-life of the photoreagents, the chromophores should not absorb in the visible region of the electromagnetic spectrum. Activation in the UVA region with photon wavelengths from  $\sim 315$ – $400$  nm is an ideal compromise. Light sources that emit in this wavelength range are readily available. This spectral window also has the advantage that the absorption spectrum of many functional groups can be easily tuned through standard application of the

Woodward–Fieser–Kuhn rules<sup>43,44</sup> for auxochromic shifting of the absorption bands of (poly)aromatic systems using common substituents.<sup>20</sup> Third, the photoconjugation process should operate in aqueous conditions and be highly tolerant to oxygen, salts, and standard components found in clinical formulation buffers that are essential to maintain protein stability. For example, high concentrations of amino acids like histidine, polysorbate, sugars, and antioxidants like sodium ascorbate are frequently used in drug formulations.<sup>45,46</sup> Fourth, the photoreagents should display high quantum yields for activation, and the bimolecular reaction kinetics with protein should be as rapid as possible to reduce the time required to produce the new bioconjugate bond. This often means optimising reaction conditions to maximise protein labelling whilst simultaneously reducing background quenching reactions including solvent mediated hydrolysis with competing water or hydroxide anions. Fifth, the bioconjugation reactions should be chemoselective and ideally site-specific.<sup>47</sup> Sixth, the new bioconjugate bonds should be stable under standard biochemical challenges (such as incubation in human serum at  $37$  °C) or else offer new options for introducing tissue-specific (typically enzyme-mediated) catabolism to facilitate drug activation and release from ADCs or metabolite excretion for radiotracers.<sup>48</sup> Finally, the methods should be amenable to automation, thereby facilitating the reproducible synthesis of protein conjugates under current Good Manufacturing Process (cGMP) conditions with high-throughput. Capturing all these features in one reagent is challenging but we find these design principles a useful starting point when screening different photoreagents for potential applications in antibody-based radiotracer development or ADC technologies.

## Practical considerations for light-induced protein conjugation: the devil is in the detail

All synthetic chemists are skilled in the use of thermally mediated reactions; however, photochemical reactions are not frequently considered as a first option in most synthetic procedures. Successful implementation of photochemical reactions in a robust and reproducible fashion involves additional experimental parameters that are not encountered when reactions are simple stirred and heated. A selection of common pitfalls that occur in synthetic photochemistry, and related practical solutions to overcome problems, is presented in Fig. 3.

Most pitfalls in photochemical reactions derive from inconsistencies in the experimental setup. Sources of error can be broadly classified into two groups that depend predominantly on either physical effects (e.g. geometry of the apparatus), or the chemistry of the process. The use of a light source is the first major difference between photochemical processes and thermally mediated reactions. Parameters associated with the light source include the wavelength ( $\lambda/\text{nm}$ ), spectral bandwidth (measured by, for example, the full-width at half-maximum,

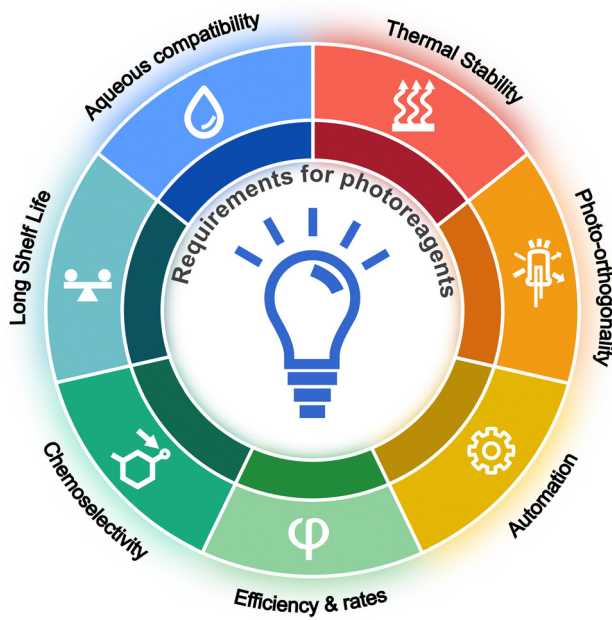


Fig. 2 Key requirements of new photoactivable reagents for applications in protein labelling.



## Common pitfalls and solutions in photochemical setups

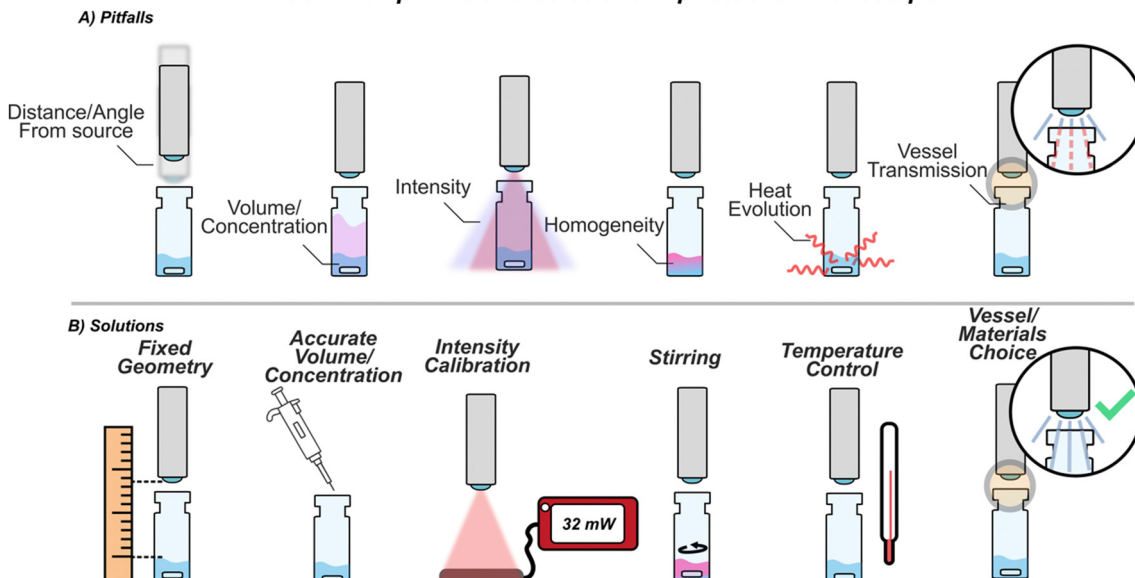


Fig. 3 Illustration of the various experimental design features of light-induced protein conjugation reactions that must be considered during reaction optimisation. (A) Common pitfalls encountered in the setup of photochemical experiments for biomolecular conjugations. Typical errors derive from inconsistent positioning of the light source, variations in reagent concentrations and total reaction volume, inhomogeneity of the sample, temperature fluctuations through heat generation or inefficient heat dissipation, and issues related to the transmission of light through materials (for example, absorption, reflection, or scattering of photons by the reaction vessel which affect photon flux). (B) Potential solutions in experimental design that improve reproducibility and overall efficiency of the photochemical process. Standardised experimental geometries are a critical requirement. In addition, the reaction composition including total volume, light intensities and shape of the light beam delivered into the reaction mixture, reagent homogeneity, temperature, and vessel materials should be tested and standardised to confer experimental reproducibility.

FWHM/nm), and power of the emission.<sup>49</sup> The beam shape, angle, distance and focal point with respect to the reaction mixture also impact the experimental geometry. Other factors include the use of either direct irradiation of the mixture or indirect irradiation through a reaction vessel (*e.g.* through glass or plastic). Indirect irradiation requires consideration of how reflectance, attenuation, scattering, and fluorescence effects from the reaction vessel impact the photon flux. Single or multi-pass geometries as well as light sources that are used either externally or internally with respect to the reaction mixture also affect the experimental design of photoreactions. On the chemical side, more common issues related to inaccuracies in reagent concentrations, the total volume of the reaction mixture, reaction homogeneity, and control of temperature can influence the success of a photoreaction. Photo-reagents may also exhibit wavelength-dependent reactivity and selectivity.<sup>49</sup> All these aspects are potential sources of uncertainty, but importantly, each can be controlled and optimised with simple precautions that are easy to implement.

The first practical aspects one must consider are the energetics and the photon wavelengths required for initiating the chemical reaction of interest. Reagents that require impractical (expensive, highly specialised, or custom-made) light sources will struggle to find widespread acceptance compared with other methods that can be initiated by using cheap, commercially available tools. For instance, high-powered light-emitting diodes (LEDs) with narrow bandwidths and peak emission at

wavelengths spanning between the UVA (365 nm) and near-infrared (NIR) spectral regions ( $\sim 1350$  nm) are readily available. These devices have long lifetimes and can produce light with well-defined characteristics. Advantages of using LEDs over common Hg-lamps or lasers include their: (i) simple and low-cost operation, (ii) wide availability around the world, (iii) generation of almost monochromatic (as well as polychromatic) light with high intensity and efficiency, and (iv) modularity and versatility with small apparatus footprints allowing them to fit inside chemical fume-hoods or glove-boxes. A collimator lens can be used for optimal beam focusing to ensure that the LED light source is directed into the reaction mixture with the most effective geometry (Fig. 4A).

Photochemical kinetics of reactions are directly influenced by the light intensity delivered to the reactants. The main contribution to the photon flux is the power output of the light source. Power output should be measured experimentally by electronic spectral radiometers or by chemical actinometry (Fig. 4B). Commercially available devices such as photodiodes, thermal power sensors, and pyroelectric energy sensors give a direct readout of the output power and represent an essential tool for a photochemistry laboratory. Practitioners should note, however, that spectral radiometers only give a threshold value to the experimental light intensity but do not account for the full impact of experimental geometry.

Chemical actinometry can provide a more accurate determination of the light intensity that inherently includes



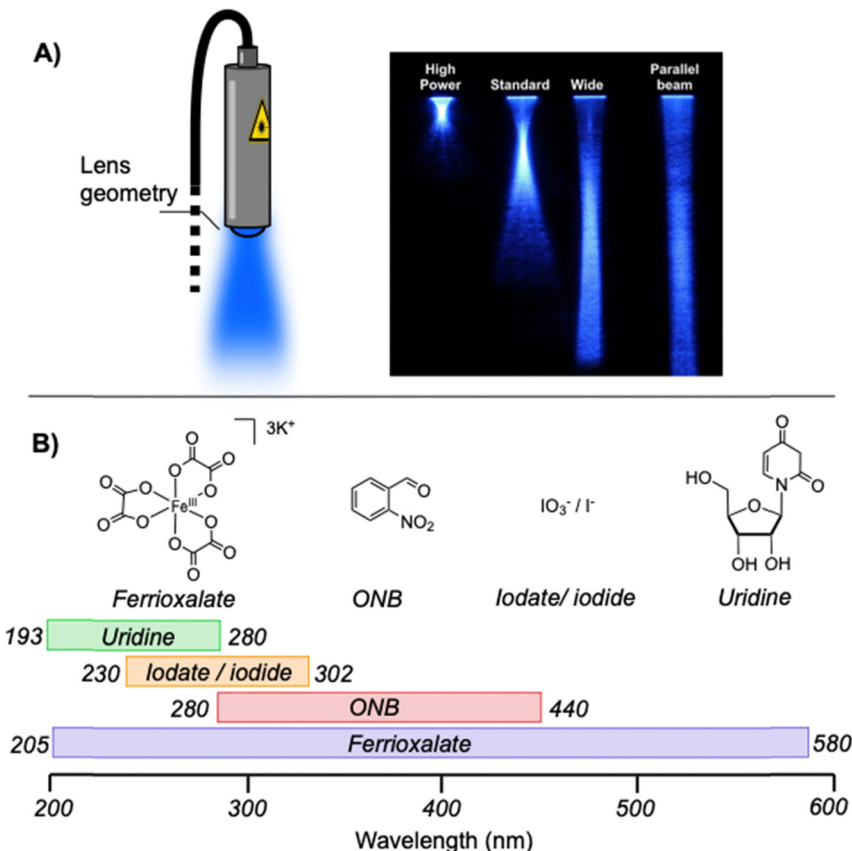


Fig. 4 (A) An illustration of LED beam configurations that can be manipulated with a lens to optimise the irradiation of a reaction mixture. (B) Examples of four chemical actinometers that span a wavelength range that is applicable for light-induced functionalisation of protein. The plot shows the spectral range for which accurate quantum yields have been reported including data on temperature and solvent dependencies for the four structures shown.<sup>50,51</sup> The image of the light beams in panel A is reproduced with permission from Opsytec Dr Gröbel, Ettlingen, Germany (<https://www.opsytec.com/>).

contributions from the experimental setup. However, actinometry can be subject to large experimental errors. Specifically, in chemical actinometry several assumptions including a fixed molar absorption coefficient and quantum yield of the actinometry reagent are required, but these may vary given changes in LED emission profiles, solvent composition, reagent concentration, and temperature. Bolton and co-workers reported extensive data on a collection of chemical actinometers, which are considered to be gold standards for calibration of photon fluxes.<sup>51</sup> Examples of chemical actinometers include ferrioxalate, uranyl oxalate, uridine, and the iodide–iodide couple (amongst others) for which detailed temperature, wavelength, and solvent dependency of quantum yields and reaction mechanisms have been reported (Fig. 4B). Another widely available chemical actinometer is *o*-nitrobenzaldehyde (ONB) which is useful for spectral regions between 280–440 nm.<sup>50</sup> The ONB compound undergoes a photoinduced rearrangement to form the corresponding *o*-nitrosobenzoic acid with well-known quantum yields. The benzoic acid has a characteristic electronic absorption spectrum which is then used to calibrate the photon flux arriving from the light source.<sup>50,52</sup>

The medium through which the light propagates from the source to the reaction mixture is also important. Direct

irradiation of the sample is the simplest design which avoids a host of complicating factors but, in some cases, closed reaction vessels or indirect irradiation through the walls of the reaction vessel are essential. The optical properties of the material used (typically borosilicate glass, quartz glass, or plastics) for the reaction vessel, as well as the vessel shape and other factors like impurities, scratches, or blemishes, influence light transmission and experimental reproducibility. For example, most chemical grade glassware is composed by borosilicate glass which filters wavelengths below 365 nm. Light sources that emit, and photoreactions that proceed, at wavelengths close to the transmission cut-off of the materials used will suffer from low reproducibility if the light is delivered indirectly through the walls of the reaction vessel. An appropriate choice of the light-guiding material and its geometry will ensure a stable and reliable photon flux during the reaction. Typically, quartz represents a good starting point as it is chemically inert and transparent to most wavelengths in the region between 300–1000 nm.

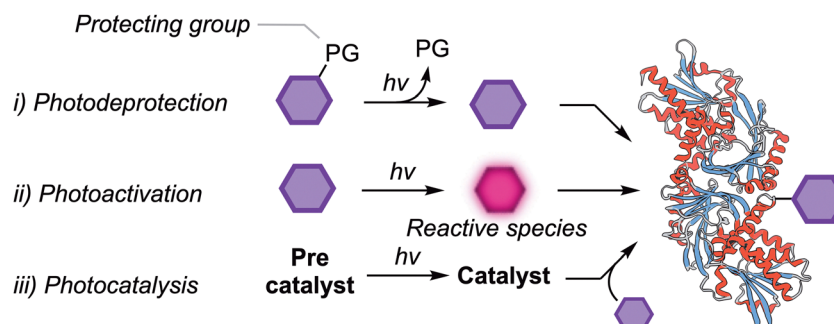
Another aspect to consider is the concentration of the reacting partners in the mixture. Optical density or turbidity can negatively impact light propagation within the sample and must be monitored. Low concentrations of the photoreagent or

protein lead to slow bimolecular conjugation kinetics and low yields of the final functionalised protein. In our experience with photo-induced labelling of humanised IgG<sub>1</sub> monoclonal antibodies (molecular weight  $\sim$ 150 kDa) or related fragments, we found that bioconjugation yields decrease rapidly if initial protein concentrations in the reaction drop below  $\sim$ 10 mg mL<sup>-1</sup> (equivalent to a concentration of  $\sim$ 67  $\mu$ M [1.5 mg of protein] in a total reaction volume of 0.15 mL).<sup>21,53-57</sup> Similarly, the stoichiometric equivalents of the photoreagent should be adjusted to ensure high conjugation yields but to avoid over functionalisation which can impinge on the biophysical properties of the protein. Typically, in our photochemical labelling reactions we adjust the initial of photoreagent-to-protein ratio by a factor associated with the conjugation yield (measured in test reactions) to ensure that on average the final protein conjugate contains a drug-to-antibody (DAR; or equivalently fluorophore or radiometal complex) ratio of 1:1.<sup>28</sup>

Sample homogeneity and thermal stabilisation can be achieved through gentle mixing by using a magnetic stir bar, but slow stirring rates (<100 rpm) and caution should be used to avoid protein foaming, flocculation, and sedimentation. Normally, the temperature of photoreactions should remain stable during the short photolysis step, but it can change if either: (i) high concentrations of chromophores are added that undergo thermal relaxation mechanisms that compete with the desired photochemical processes, (ii) reactions involve strongly exothermic steps, or (iii) the LED source generates heat. Heat sinks, heating mantles or jacketed reaction vessels can be used in situations where tight control over temperature is essential.

## Mechanistic classifications of light-induced protein conjugation reactions

In this section, we subdivide the reactivity of photoreagents into three different classes based on their mechanisms of action involving: (i) photodeprotection of masked reagents, (ii) photoactivation to generate highly reactive intermediates, and (iii) photocatalysis (Scheme 2).



**Scheme 2** Bimolecular photoconjugation strategies categorised into three distinct mechanisms depending on the role of the photoactivatable reagent. Mechanism (i) involves the activation of masked functional groups by release of a photolabile protecting group (PG) to give an intermediate that subsequently reacts with protein. Mechanism (ii) involves light-induced activation of a stable ground-state reagent to form an unstable intermediate which is the main protagonist in the bioconjugation reaction. Mechanism (iii) involves photocatalytic reactions in which a photosensitive precatalyst activates by absorption of a suitable photon and promotes reactivity of a substrate in the bioconjugation step.

Photodeprotection reactions are a mainstay of photochemistry and the topic has been reviewed extensively.<sup>58,59</sup> Despite appearing to be similar, the photodeprotection and photoactivation mechanisms (Scheme 1, mechanisms i and ii, respectively) are conceptually and empirically distinct. Specifically, photodeprotection reactions generate a stable intermediate which is only reacts in the presence of the corresponding reaction partner. An example is the release of a bioorthogonal reactive strained alkyne upon light-mediated CO release from dibenzocyclopropenones (see below).<sup>60,61</sup> These types of reaction are attractive when spatial and temporal control is required over the location of light-induced protein tagging, particularly in labelling components of live cells.<sup>62-67</sup>

In contrast, photoactivation (Scheme 1, mechanism ii) produces very unstable, highly reactive, and transient intermediates that react on the picosecond-to-microsecond times scale. Examples of photoactivatable reagents include tetrazoles, azirines, sydnone,<sup>68</sup> benzophenones, aryl and aliphatic diazirines, diazo-species, and aryl azides, which undergo photochemical reactions *via* an electronically excited state. These photochemical reactions transit through highly reactive species including carbenes, nitrenes, biradical species, electrophiles like ketenimines and dipolar species such as nitrile imines and nitrile ylides. In spite of the extreme reactivity of these photoreagents, many compounds have been used in PAL.<sup>33,69-84</sup> In the third mechanistic group, (Scheme 1, mechanism iii), the photocatalytic process depends on an initial activation of an additive (a precatalyst) which upon photon absorption, mediates a bioconjugation reaction between a substrate and a protein of interest. The following sections highlight examples of photoreagents which have been employed in the synthesis of functionalised protein conjugates.

## Photoreagents and their applications

The following sections summarise the chemistry of eleven of the most prominent photoreagents for direct (bimolecular) functionalisation of proteins. For recent complementary reviews on photochemical reactions and their applications to



create bioactive molecules, especially with photo-click reactions, the reader is referred to ref. 58, 85 and 86.

## Aryl azides

Aryl azides ( $\text{ArN}_3$ ) are one of the most well-studied compound classes for photoconjugation chemistry.<sup>87</sup> Their development as photoreagents date back to 1969 when Fleet *et al.*<sup>30</sup> used 4-fluoro-3-nitrophenylazide for labelling antibodies, and later this class of compounds was used in PAL.<sup>69,70,78–81,88–90</sup> Recently, our group adapted  $\text{ArN}_3$  chemistry for the *photoradiosynthesis* of antibody-based radiotracers using a wide range of radioactive nuclides including (amongst others)  $^{89}\text{Zr}$ ,  $^{68}\text{Ga}$ , and  $^{64}\text{Cu}$  for positron emission tomography (PET; Scheme 3).<sup>21,53,54,56,91</sup> In our hands, the chelating reagents derivatised with the  $\text{ArN}_3$  functional group display thermal stability up to  $\sim 50$  °C, are stable over prolonged periods of time ( $> 2$  years) in the freezer at  $-20$  °C. Aryl azides have the advantage that they can be readily installed onto complex drug molecules, fluorophores, or radiometal complexes. Their high chemical stability in buffered aqueous media, and biocompatibility with formulated antibody mixtures, combined with convenient and rapid photochemical activation with photons in the wavelength range 365–450 nm make them close to ideal photoreagents for protein labelling. Upon light-absorption, the  $\text{ArN}_3$  group is promoted to an electronically excited (singlet) state in which the rapid and almost barrierless extrusion of  $\text{N}_2$  is favoured, generating highly reactive open-shell singlet nitrenes.<sup>87,92</sup> Experimental measurements indicated that the quantum yield of  $\text{ArN}_3$  activation in water is  $\sim 4\%$ .<sup>21</sup> Depending on the electronic nature of the substituents on the aryl ring, the aryl nitrene may react either as a nitrene species or undergo rapid intramolecular bicyclisation then ring opening to form a potent 7-membered ketenimine heterocycle, which acts as a chemoselective electrophile for primary amines.<sup>92</sup> Chemoselective coupling of the ketenimine with a lysine side-chain on protein produces a 2-aminoazepine which acts as a stable bioconjugate bond *in vivo*.<sup>62,91</sup>

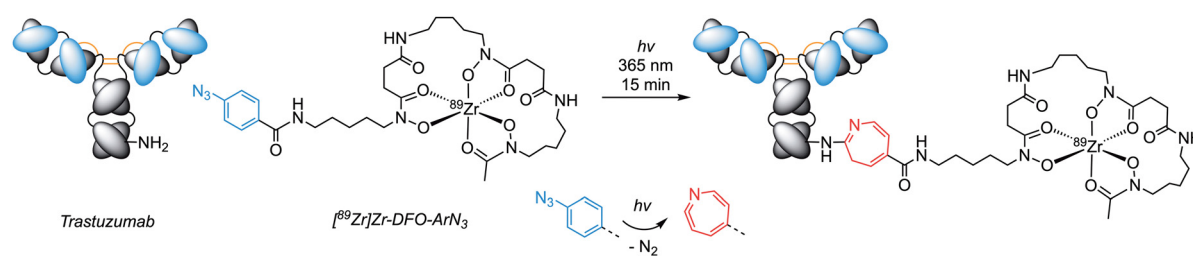
In one example, we used  $[^{89}\text{Zr}]\text{ZrDFO-}\text{ArN}_3$  (DFO, desferrioxamine) to photoradiolabel a monovalent engineered antibody onartuzumab with high radiochemical conversions ( $\sim 57\%$ ) and isolated decay-corrected radiochemical yields ( $\sim 41\%$ ) of  $^{89}\text{Zr}$ -onartuzumab.<sup>91</sup> The photoradiolabelled  $^{89}\text{Zr}$ -onartuzumab

was then tested in cells and in mice bearing human gastric cancer models comprised of subcutaneous human hepatocyte growth-factor receptor (c-MET) overexpressing MKN-45 xenografts. PET imaging, biodistribution, and pharmacokinetic studies revealed superior performance of the photoradiolabelled compound when compared head-to-head against a control  $^{89}\text{Zr}$ -onartuzumab radiotracer formed by using the standard DFO-Bn-NCS<sup>93</sup> bioconjugation approach that forms a thiourea.<sup>91</sup> Notably, the  $\text{ArN}_3$  photochemistry was found to be compatible with several different clinical formulation buffers. This advance also led to the design of a new radiosynthesiser for automated light-induced synthesis of immunoconjugates (ALISI).<sup>54</sup>

## Tetrazoles

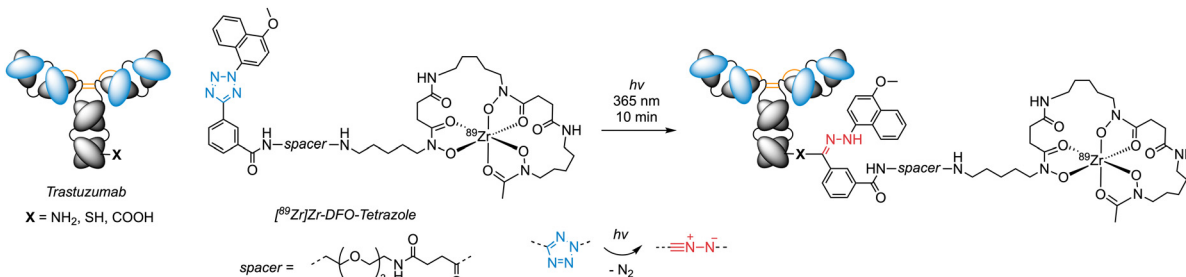
The photochemistry of tetrazoles was originally discovered by Huisgen and co-workers in 1967 where evidence of photoinduced cycloadditions between the heterocycle and ethyl crotonate were reported.<sup>94</sup> At that time, and in subsequent studies,<sup>31,95,96</sup> it was noted that cross-reactivity between photoactivated tetrazoles with biologically relevant nucleophiles occurs but this fact was subsequently overlooked when tetrazoles and alkene-substituted proteins were combined to develop 'photo-click' chemistry in 2008.<sup>97,98</sup> Photo-click reactions with tetrazoles were proclaimed to be bioorthogonal but the original report,<sup>94</sup> and detailed mechanistic studies in 2016<sup>99,100</sup> refuted this claim. Indeed, studies have demonstrated photoinduced reactivity of tetrazoles with a wide range of reagents<sup>99</sup> with reports of high selectivity towards amino<sup>101</sup> carboxyl<sup>102,103</sup> thiol<sup>104</sup> alkene, alkyne<sup>105</sup> and other functionalities,<sup>106</sup> depending on the conditions employed. Our own *photoradiosynthesis* experiments with a novel  $[^{89}\text{Zr}]\text{ZrDFO-tetrazole}$ <sup>20</sup> complex for light-initiated labelling of trastuzumab also confirmed that direct protein functionalisation occurs (Scheme 4).<sup>20</sup> Similar to the work on  $\text{ArN}_3$  species, we showed that tetrazole photochemistry is a viable route for synthesising bioactive radiotracers for applications in PET imaging.<sup>20</sup>

Upon irradiation with UV light, the electronically excited state of tetrazoles undergoes a stepwise rearrangement and photodissociation.<sup>92</sup> First, a weak N–N bond breaks to form an electronically excited intermediate which then undergoes



**Scheme 3** Photoradiosynthesis to label a monoclonal antibody with a positron-emitting  $^{89}\text{Zr}$ -desferrioxamine complex via light-induced activation of a  $\text{ArN}_3$  group. Trastuzumab is linked in a one-pot photoreaction to  $[^{89}\text{Zr}]\text{ZrDFO-}\text{ArN}_3$  with high isolated and decay-corrected radiochemical yields and radiochemical purities.<sup>28,53,54</sup>





**Scheme 4** Photo(radio)synthesis of functionalised proteins using light-induced activation of tetrazoles. Formation of the electronic excited state of a tetrazole can lead to intramolecular rearrangements and loss of  $N_2(g)$  to generate a 1,3-dipolar nitrile imine. This intermediate finds applications in labelling compounds bearing alkene or alkyne reaction partners (photo-click) or in direct reaction with biologically relevant nucleophiles found on protein.

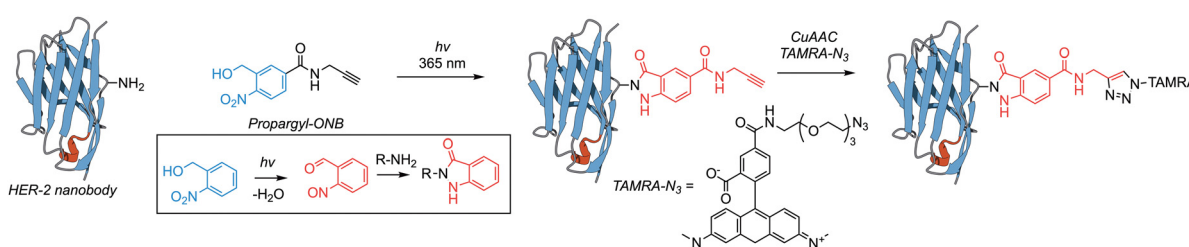
spontaneous and rapid loss of  $N_2$  to form a nitrile imine. Nitrile imines undergo fast 1,3-dipolar cycloaddition reactions with alkenes and alkynes,<sup>92</sup> but also react with a wide variety of biologically relevant nucleophiles. Remarkable examples of their applications are the on-protein synthesis of fluorogenic groups by Qing Lin and co-workers,<sup>63,97,107–109</sup> fluorescence microscopy imaging,<sup>110,111</sup> and radioimmunoconjugate photosynthesis.<sup>20,92</sup>

Photolysis of tetrazoles at wavelengths that do not lead to photodegradation of protein requires auxochromic tuning of their absorption spectrum.<sup>20</sup> To this end, our group developed naphthyl tetrazole derivatives and performed structure–activity relationship experiments.<sup>20</sup> Introduction of a methoxy group onto a naphthyl-tetrazole facilitated rapid and efficient photoactivation at wavelengths between 365 to 395 nm. Detailed computational studies also suggested that the reactivity of tetrazoles with biological nucleophiles might be exploited in future studies by using different experimental conditions to tune the chemoselectivity.<sup>92</sup> Overall, tetrazoles are one of the most synthetically versatile classes of photoreagent for labelling proteins.

## ortho-Nitrobenzyl alcohols (ONBAs)

The photochemical behaviour of nitroso compounds was first reported in 1901 when the pioneers of photochemistry Ciamician and Silber<sup>112</sup> described the photoinduced rearrangement to *o*-nitrobenzaldehyde to *o*-nitrosobenzoic acid photolysis.<sup>112</sup>

Other important works on photochemical reactions of *o*-nitrobenzyl alcohols (ONBA) and related derivatives were written by Sachs in 1904<sup>113</sup> where it was predicted that, “*All aromatics which have a hydrogen ortho to a nitro group will be light sensitive.*”<sup>114</sup> Later in 1970, Woodward and co-workers used ONBAs as photo-removable protecting groups for amino-, carboxy- and ester groups.<sup>115</sup> The usefulness of ONBAs and derivatives as photoprotecting groups has been extensively studied by the group of Bochet.<sup>59,116–122</sup> Upon photon absorption, ONBAs undergo an intramolecular redox reaction generating the corresponding *o*-nitrosobenzaldehyde, which until recently, has been exploited mainly for photochemical deprotection of reactive groups. The group of Xiao-Hua Chen repurposed ONBAs for the *in situ* conjugation of proteins (Scheme 5).<sup>123</sup> Here, the photogenerated *o*-nitrosobenzaldehyde is susceptible to nucleophilic attack from primary amines, condensing to give the corresponding indazolones after intramolecular cyclisation.<sup>123,124</sup> This reactivity enables the use of ONBAs as chemoselective photochemical linkers between the  $\epsilon$ -NH<sub>2</sub> of lysine side-chains and the photogenerated *o*-nitrosobenzaldehyde. Photochemical conjugation experiments with ONBAs were demonstrated on a wide range of substrates spanning from simple amines and peptides, through to nanobodies. In one study, a nanobody that binds to the human epidermal growth factor receptor type 2 (HER2) was photochemical derivatised by using an alkynyl derivative of ONBAs. Mass spectrometric analyses conducted by MALDI-TOF revealed lysine-specific and near quantitative protein labelling. The ONBA-derived probes were also activated in live cell cultures by UV light (365 nm) and enabled precise temporal and spatial control of bioconjugation, with



**Scheme 5** Schematic representation of the light-induced ONBA reaction mechanism labelling a HER2-specific nanobody.<sup>123</sup> (Step 1, left) Photoinduced ONBA activation and chemoselective protein derivatisation with an alkynyl group. (Step 2, right) The formation of a covalent bond between the protein and the modified probe via Cu<sup>1</sup>-mediated alkyne–azide click chemistry, illustrating successful bioconjugation towards TAMRA-N<sub>3</sub>.



minimal cellular toxicity. The ONBA strategy enabled kinase profiling in live mammalian cells where a lysine-reactive probe captured over 90 kinases in Jurkat and 76 in K562 cells, outperforming diazirine probes. Structural docking confirmed the selectivity of the probe for conserved lysine residues in kinase ATP-binding sites. The same methodology was also expanded to include mitochondria-specific labelling with a fluorescent rhodamine-ONBA probe.

## Diaryl sydnone

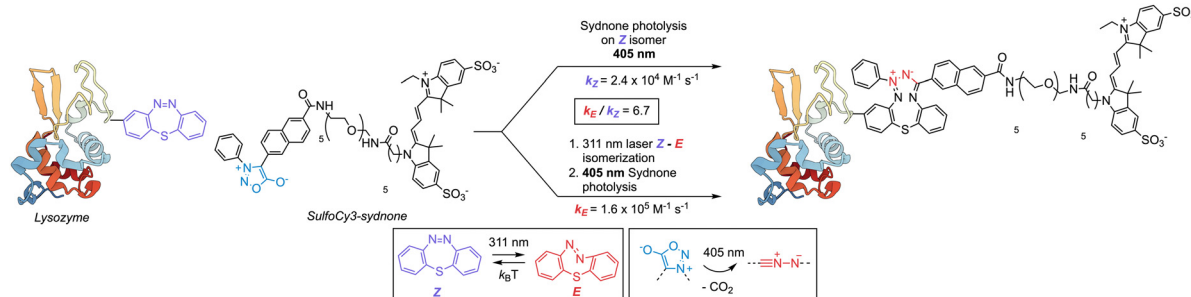
The photoactivity of sydnone was established in 1955 when Tien and Hunsberger reported the synthesis of their pyridyl derivatives which displayed solid-state photochromic behaviour when exposed to sunlight.<sup>125</sup> The transparent crystals turned dark blue under light and the transition was reverted by heating or by leaving the crystals in the dark for prolonged times. More recently, Taran and co-workers experimented with the use of sydnone in copper-mediated cycloadditions to alkynes,<sup>126</sup> and then further improved strategies were proposed for strained alkynes.<sup>127,128</sup>

The photochemical reactivity of sydnone derivatives on biomolecules came later. In 2018 the group of Zhipeng Yu synthesised a library of diaryl sydnone aiming to tune the electronic structure of these compounds to absorb and react at wavelengths more compatible with applications in biochemistry.<sup>129</sup> Their proposed working mechanism resembles the one of tetrazoles.<sup>130</sup> Photon absorption by the sydnone group creates an electronically excited state which releases  $\text{CO}_2$  and forms a nitrile imine. As a consequence, the reactivity patterns of sydnone are anticipated to be comparable to tetrazoles. Initial studies demonstrated that lysozyme, pre-functionalised with strained alkynes, undergoes efficient photo-induced and fluorogenic labelling.<sup>131</sup> Similar reactivity was observed with strained alkenes (e.g. *trans*-cyclooctene, TCO), which undergo fluorogenic cycloadditions with the sydnone-generated nitrile imines forming the corresponding pyrazolines. The pyrazoline products display efficient luminescence properties with high fluorescence quantum yields (0.28 to 0.42) and turn-on enhancement factors (122 to 321-fold).<sup>129</sup>

The magnitude of these turn-on effects allows for straightforward monitoring and quantification of protein labelling and enables sensitive detection of protein conjugates at sub-micromolar levels.<sup>129</sup>

Sydnones also undergo cycloaddition reactions *via* their nitrile imine intermediate with dibenzo-thiadiazepine (DBTD) reagents (Scheme 6).<sup>64,132</sup> Notably, dibenzo-thiadiazepines display concomitant photo-isomerisation where the less stable *E*-isomer was shown to react faster with the nitrile imine. Kinetic studies highlighted that the nitrile imine displayed considerable rate enhancements toward the *E*-isomer of the DBTD compound which are attributed to increased ring strain ( $k_E = 1.6 (\pm 0.16) \times 10^5 \text{ M}^{-1} \text{ s}^{-1}$ ,  $k_Z = 2.4 (\pm 0.24) \times 10^4 \text{ M}^{-1} \text{ s}^{-1}$  for *Z*,  $k_E/k_Z = 6.7$ ). The interaction of sydnone with DBTD is also fluorogenic, thereby facilitating quantification of the protein conjugation step *via* fluorescence emission coupled to gel electrophoresis methods for protein separation. Photolabelling reactions with a sulfo-Cy3 fluorophore diaryl sydnone derivative exhibited successful bioorthogonal ligation of lysozyme or bovine serum albumin (BSA) where the protein was pre-functionalised with a DBTD reagent.<sup>132</sup> Although potentially versatile, current applications of photolabelling chemistry with these DBTD-sydnone reagent pairs remains complex. For instance, the setup requires two light sources for triggering the formation of the nitrile imine at 311 nm and the *Z*-*E* photo-isomerisation (quantum yield for isomerisation:  $\Phi_{ZE405} = 0.516$  at 298 K) of the DBTD partner at 405 nm using laser light sources. A notable advantage is that the DBTD reagent has excellent stability in the biochemical environment and is resistant to photodegradation (9.4% bleaching after 3500 light-dark cycles). However, rapid thermal reversion from the *E*-to-*Z* isomer ( $3.75 \pm 0.23 \text{ s}^{-1}$ , 298 K) generates a very narrow reaction window of only a few seconds. This can provide high control over the generation of the reactive intermediate but simultaneously limits the accessible reactive space for bimolecular protein conjugation to only extremely fast bioorthogonal partners.

Importantly, the sydnone-DBTD technology has been applied in live cells by *in situ* labelling of cetuximab<sup>131,132</sup> and panitumumab<sup>132</sup> derivatives bearing dibenzothiadiazepine.



**Scheme 6** Diaryl sydnone eliminate  $\text{CO}_2$  under light irradiation forming reactive nitrile imines. In this example a thiadiazepine functionalized lysozyme undergoes photoinduced (405 nm) cycloaddition to the photogenerated nitrile imine with a rate constant  $k_E$ . The cycloaddition rate constant increases by  $k_E/k_Z = 6.7$  times following a stepwise procedure in which the diazepine is first converted to the *Z* geometric isomer. In the subsequent step, the nitrile imine is generated *in situ* by irradiation with 405 nm light, thus initiating protein conjugation to the Cy3-sydnone derivative.<sup>132</sup>



Fluorescence microscopy revealed that irradiating the cell sample with 405 nm resulted in Cy3 accumulating on the cell surface.<sup>132</sup> In conclusion, sydrones are promising photoreagents with future prospects for developing both bioorthogonal tools and for potential direct protein conjugation.

## Diaryl azirines

The photochemistry of azirines was first reported in 1968 by Arnold<sup>133</sup> and later in the 1970s by Padwa<sup>31,32</sup> who used these reagents as photochemical building blocks. The main application of diazirines lies in their ability to produce nitrile ylides *via* photo-induced ring-opening rearrangements.<sup>134</sup> Nitrile ylides have been used as cycloadditions reaction partners with dienes or dipolar compounds.<sup>134</sup> However, the use of azirines in bioconjugation chemistry remains relatively unexplored. Computational studies have predicted that nitrile ylides display activation parameters which point toward faster reactivity compared with nitrile imines generated from tetrazoles or sydrones.<sup>135</sup> This is in line with significantly lower activation free energies for 1,3-dipolar cycloadditions and was corroborated experimentally by their preference to react with unsaturated dicarbonyl compounds bearing electron-withdrawing substituents.<sup>135,136</sup>

Light-induced activation of the 3-membered azirine ring typically requires photons with short wavelengths around 300 nm. Consequently, their application in photoinduced bioconjugation chemistry has been limited. To alleviate this drawback, Barner-Kowollik and co-workers substituted one of the aryl groups with a pyridyl group to redshift the activation wavelength to 405 nm.<sup>137</sup>

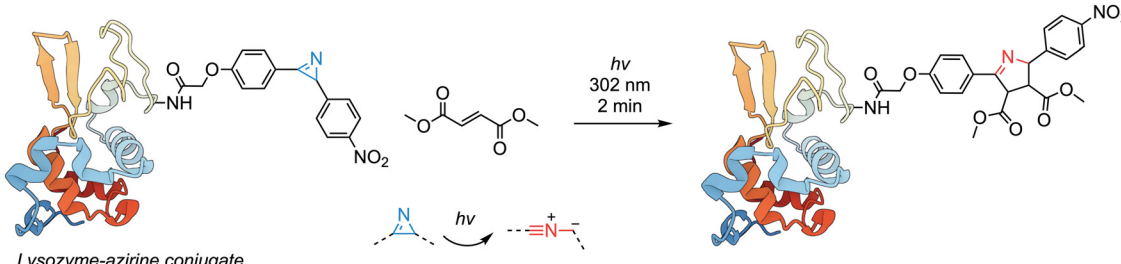
Lin and co-workers prepared azirine-functionalised lysozyme (*via* classic NHS conjugation methods).<sup>136</sup> The bioconjugate then underwent 302 nm photon absorption and a light-induced reaction with unsaturated 1,4-dicarbonyl compounds such as dimethyl fumarate or a PEG-ylated derivative of fumarate (Scheme 7). Successful protein labelling was reported, and the reaction shows characteristics of a bioorthogonal process, but further work is required to establish azirine photochemistry as a reliable method for protein functionalisation. In particular, issues related to the use of high-energy photons, the necessity to introduce the photoactive group *via* a non-bioorthogonal

step, and the slow photoreaction kinetics (photoreaction rate constant of  $0.03\text{ s}^{-1}$  using a 20-fold excess fumarate)<sup>136</sup> must be addressed before diaryl azirines can become a more widely used class of photoreagent for protein conjugation.

## Photodeprotection of strained alkynes

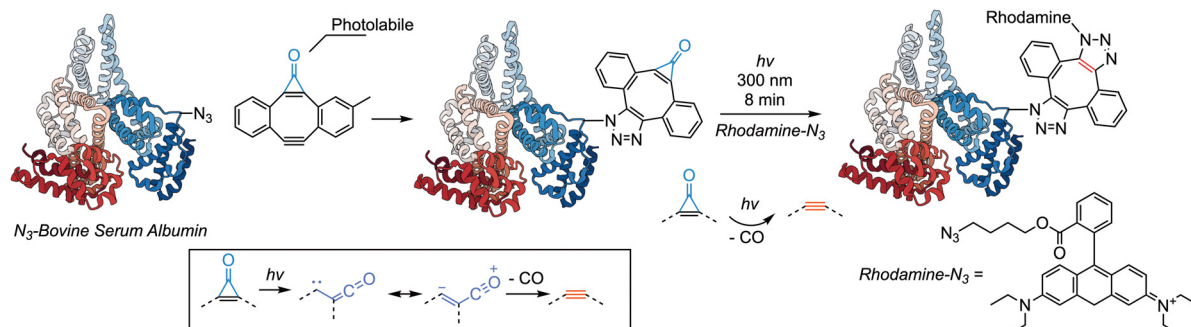
Strained alkynes have been central to the development of click chemistry for biological applications.<sup>138–140</sup> Recently, a new generation of photo-protected strained alkyne reagents has expanded the photochemical reaction palette with cyclopropanes being the most prominent members.<sup>67</sup> In 2009, Popik and co-workers reported a novel application involving these compounds and demonstrated their utility for labelling biomolecules in challenging situations such as those involving intact cells.<sup>67</sup> The photolysis of the 3-membered cyclic enone results in the rapid generation of the strained alkyne, which serves as an ideal substrate for strain-promoted azide–alkyne cycloadditions (SPAAC).<sup>141</sup> Following the formation of the alkyne, the introduction or concurrent presence of an azide derivative initiates the SPAAC reaction, leading to the synthesis of the corresponding triazole with bimolecular rate constants around  $0.05\text{ M}^{-1}\text{ s}^{-1}$  (measured in MeOH; for comparison, typical values for SPAAC on unprotected alkynes are  $\sim 0.1\text{ M}^{-1}\text{ s}^{-1}$  in  $\text{H}_2\text{O}$ )<sup>140,142</sup> Subsequent experiments showed that the photodecaging and SPAAC approach can be employed to label intact Jurkat cells supplied with *N*-azidoacetyl-sialic acid.<sup>67,143</sup> This supplement leads to the selective incorporation of azido groups in glycoproteins and glycolipids synthesised by the cells, thus providing a suitable bioorthogonal substrate for evaluating photodecaging reactivity of alkynes in living systems. For example, azide-presenting cells were subsequently exposed to ultraviolet light in the presence of a cyclopropenone-biotin conjugate, initiating the formation of triazole linkages between biotin fragments and cellular proteins. Incubation of the biotin-functionalised cells with an avidin-Alexa Fluor 488 conjugate showed efficient labelling as detected by using fluorescence microscopy.<sup>67</sup>

The CO-releasing reaction on cyclopropanes has been analysed in detail through a combination of DFT calculations and flash photolysis experiments which probed the nature of the decarbonylation step.<sup>60</sup> Electronic transitions responsible



**Scheme 7** Diaryl azirines undergo photoinduced ring-opening reactions to form nitrile ylides, which are established reaction partners for cycloaddition reactions. Here, photolysis of a pre-functionalised lysozyme-diazirine derivative with 302 nm light, stimulates the formation of a new conjugate bond with electron-poor dienes (such as methyl fumarate), forming the cycloaddition product.<sup>136</sup>





**Scheme 8** Cyclopropenones are photolabile compounds that undergo decarbonylation reactions upon irradiation. Photochemical CO extrusion leads to the formation of the corresponding alkyne. Specifically, for the dibenzocyclopropenone-derivatives the unmasked alkyne lies within a strained ring system, thereby facilitating classic bioorthogonal click reactions. In this example, an initial SPAAC is performed to connect an  $\text{N}_3$ -derivative of bovine serum albumin (BSA) to the cyclopropenone. This protein conjugate is then photolytically decarbonylated to expose the alkyne, which is used in a second SPAAC reaction to bridge the protein to rhodamine fluorophore.<sup>61</sup>

for the fragmentation of the molecule have been identified, and mechanistically, the loss of CO is proposed to occur in a stepwise fashion. First, the cyclopropenone undergoes an energy-demanding ( $\sim 134 \text{ kJ mol}^{-1}$ ) ring-opening reaction by forming a ketenylcarbene intermediate (Scheme 8). The ketenylcarbene can be described by two resonance structures, one of which is neutral (carbene form) and the other displays charge separation (zwitterionic form). This intermediate then undergoes fast decarbonylation, highlighting the low activation barrier to cleave the remaining C-CO bond. From the analysis of the computational and experimental results, it was hypothesised that CO release happens in an electronically excited state of the zwitterionic intermediate, as supported by intense solvent polarity effects observed during kinetic experiments.<sup>60</sup> An illustration of the photolabelling of proteins with cyclopropenones is presented in Scheme 8.<sup>61</sup>

Upon photodeprotection, cyclopropenones also become suitable reagents for inverse electron demand Diels–Alder (IEDDA) reactions.<sup>144</sup> In this framework, 1,2,4,5-tetrazine species reacts with a dienophile like a strained alkene or alkyne through a classic [4+2] cycloaddition pathway. The cycloaddition is accompanied by a concomitant release of nitrogen which represents the driving force of the reaction. As discussed above, the alkyne can be generated *in situ* from the photolysis of a dibenzocyclopropenone, which converts into the corresponding cyclooctyne and then participates in an IEDDA reaction. A remarkable example of this technology has been presented by the Lang group, in which protein engineering was adopted as a biosynthetic strategy to introduce site-specifically tetrazine modified versions of lysine on a variety of proteins including superfolder green fluorescent protein (sfGFP).<sup>144</sup> The tetrazine-modified sfGFP was tested for reactivity toward masked alkynes, which yielded nearly quantitative photoreactions upon exposure to light. This system was then further tested on living *E. coli* samples demonstrating photochemical labelling of intact cells. Protected strained alkynes represent an exemplary case of photoinduced deprotections (Scheme 1, mechanism i), which introduce an additional dimension to synthetic biochemistry.

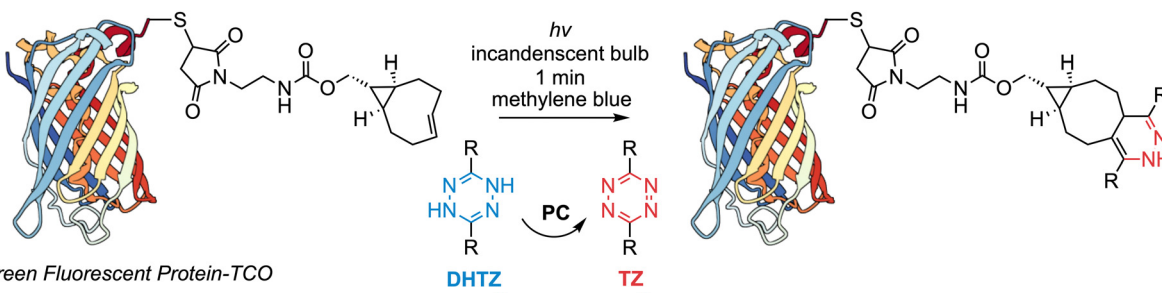
## Photoactivation of tetrazines

Related to the chemistry discussed in the previous section, tetrazines have been used extensively in IEDDA reactions on biological substrates, including for pretargeted *in vivo* labelling applications in the space of radiotracer imaging and therapy.<sup>65,145–149</sup> The tetrazine chemistry and IEDDA reactions have been the subject of numerous excellent reviews, but the majority of the work addresses only thermally-mediated processes.<sup>150–152</sup> Light-activated tetrazine chemistry has been reported with activation mechanisms spanning both photoprotective and photoredox processes (Scheme 1, mechanisms i and iii, respectively).

In 2016, Fox and co-workers reported the use of catalytic turn-on photooxidations for converting inactive dihydrotetrazines (DHTZ, Scheme 9) into reactive tetrazines (TZ) under LED irradiation at 600 nm.<sup>153</sup> The photooxidation mechanism exploits the sensitising properties of compounds such as methylene blue, rose bengal, and carboxyfluorescein, which act as photocatalysts for the oxidation of DHTZ into TZ. Methylene blue and rose bengal are known as photosensitisers to produce singlet oxygen ( ${}^1\text{O}_2$ ), and initial speculations suggested that this species could be the effective oxidant.<sup>153</sup> This hypothesis was disproven by conducting control experiments in the presence of  $\text{NaN}_3$  (a  ${}^1\text{O}_2$  quencher)<sup>154,155</sup> thus showing that the photocatalytic effect was independent from the formation of reactive oxygen species.

These observations led to the conclusion that the photooxidation of DHTZs represents a practical protocol for developing biocompatible functional materials and for the photoinduced formation of protein conjugates. Similar strategies have been employed in other works from the same group in which additional protein derivatives have been photolabelled by using the DHTZ/TZ dyad.<sup>66</sup> These preliminary reactions on model proteins served as the foundation for subsequent development of live-cell imaging agents.<sup>66</sup> Indeed, the strategy devised by Fox and co-workers facilitates rapid and spatiotemporally resolved labelling of engineered proteins expressed by cells, hence opening new avenues for understanding fundamental biochemical processes.





**Scheme 9** The photocatalytic oxidation of DHTZ is useful for generating tetrazines on demand, which are potent substrates for bioorthogonal IEDDA-type reactivity *in vitro* and *in vivo*. In this example, green fluorescent protein (GFP) was functionalised with a strained *trans*-cyclooctene (TCO) by using a thiol–maleimide conjugation. Subsequent incubation with a DHTZ reagent, followed by photocatalysed oxidation to unmask the TZ partner led to successful protein functionalisation.<sup>153</sup>

Forsythe and co-workers applied these concepts in the design of biocompatible and nontoxic materials which can be used *in vivo*.<sup>156</sup> The advantages derived from these methodologies are the short times of photoreaction, red-shifted wavelengths, and the widespread availability of the photocatalysts.

Tetrazine reagents have also been employed in photodeprotection strategies. For instance, Devaraj and colleagues demonstrated tetrazine release from a photocaged dihydrotetrazine, which included a photoprotecting group akin to *o*-nitrobenzyl carbamates that can be removed by exposure to 425 nm light. The short irradiation times (less than 2 minutes), in conjunction with the high reaction rates and red-shifted absorption, render this methodology a particularly advantageous approach for on-demand biomolecule derivatisation.<sup>62</sup>

In summary, the development of photooxidation-based protocols for DHTZs and tetrazine derivatives presents a powerful approach for biocompatible material synthesis, live-cell imaging, and on-demand biomolecule modification. These advances, characterised by rapid reaction rates, tunable wavelengths for photoactivation, and the availability of photocatalysts, open new avenues in biomedical research and offer innovative tools for studying and manipulating biochemical processes with high spatial and temporal precision.

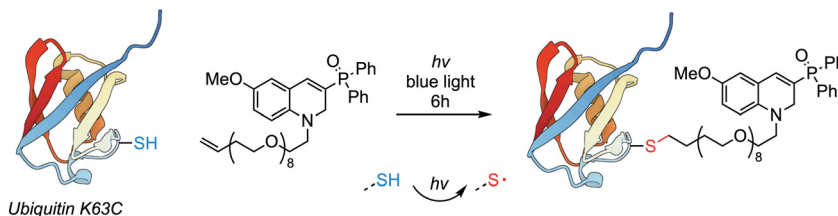
## Thiol–ene reagents

The distinctive chemistry of sulfhydryl groups (redox chemistry, variable  $pK_a$  values, photoreactivity, high nucleophilicity and soft Lewis base class B character), coupled with their widespread availability on biomolecules, present an exceptional opportunity of using this functional handle in novel photochemical processes. Most of their thermally mediated chemistry relies on the acid–base properties of the SH group and takes advantage of their innate nucleophilicity. Photochemical reactions between terminal mercaptans and alkenes have been known for more than a century<sup>157</sup> but in recent years there has been a ‘rediscovery’ of R-SH chemistry for applications in direct bioconjugation of protein. In their light-induced reactions, thiols become activated and generate thiyl radicals ( $RS^\bullet$ ).

These high-energy intermediates react readily with alkene substrates frequently following anti-Markovnikov patterns,<sup>158</sup> although the Markovnikov addition products are observed in rare examples.<sup>159</sup> Radical reactivity poses an immense challenge to control, especially on biological substrates under aqueous aerated conditions. Photochemical thiol–ene reactions are not immune from these drawbacks but efforts have been made to mitigate and tame the reactivity of these systems. Numerous research groups have explored the creation of masked thiols including derivatives of coumarin or *o*-nitrobenzyl which photolytically fragment and release the free thiol.<sup>59,160,161</sup> Although the thiol–ene and related thiol–yne reactions display potential in biomolecule functionalisation, the technology needs to mature before it can find broader applications. One issue that must be addressed is that the production of highly chromophoric products after the photodeprotection can impede the efficiency of the thiol–ene reaction. Specifically, these highly absorbing byproducts accumulate within the reaction mixture and progressively function as light filters, consequently impinging the overall efficacy of the reaction.<sup>162,163</sup> Controlling the conditions to minimise competing reaction pathways like radical quenching is also essential to improve bioconjugate yields to useful levels.

Encouragingly, the group of Sungwoo Hong developed a photochemical system that features mild activation parameters, high selectivity, and biocompatibility. In this work, they prepared a novel generation of quinoline-based photosensitisers poised to activate cysteine side-chain thiols at wavelengths around 440 nm.<sup>85</sup> Detailed mechanistic investigation on the thiol–ene reaction confirmed the involvement of radical species, where radical scavengers such as TEMPO (2,2,6,6-tetramethylpiperidine-1-oxide) completely inhibited the formation of the desired products. This reactivity has been exploited for the site-selective formation of thioether bonds on bovine serum albumin (BSA) and ubiquitin K63C (Scheme 10), a version of ubiquitin displaying substitution of lysine 63 for a cysteine residue. Modified variants of these proteins have been synthesised by the thiol–ene method and feature, for instance, a biotin pendant arm or a quinoline derivative reminiscent of the photocatalysts discussed above.





**Scheme 10** Thiol–ene reactions proceed through the formation of a photo-generated thiyl radical which is particularly reactive towards unsaturated compounds, such as alkenes or alkynes. In this example, a photosensitised version of the thiol–ene reaction is triggered by 440 nm irradiation to create a new thioether bond bridging a quinoline derivative to ubiquitin-expressing cysteine in position 63.<sup>85</sup> Interestingly, the substrate also acts as the photosensitiser, promoting the bioconjugation reaction and producing a fluorescent protein conjugate.

In the latter example, the small-molecule reagent served a dual role acting as both the photocatalyst and the alkene source by initiating the thiol–ene reaction and ultimately conjugating with the protein (Scheme 10). Such a strategy provides a convenient instrument for a site-selective, photochemical, and single-step introduction of a fluorophore subunit on proteins that display accessible thiols.

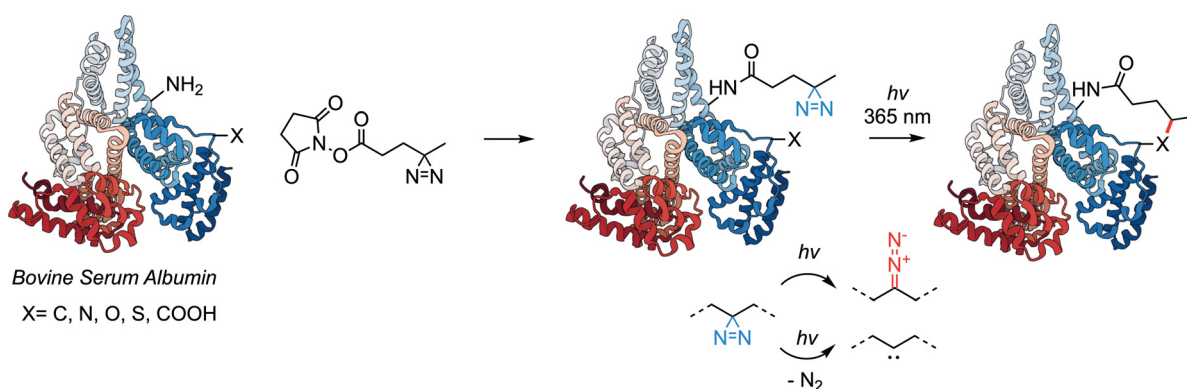
## Diazirines

Diazirines quickly found applications as PAL probes<sup>75,76,164</sup> in biochemistry in the 1970s when Knowles and co-workers exploited their photochemical reactivity for biomolecule labelling.<sup>34,35,165</sup> Their productive photochemistry involves electronic excitation of the diazirine group through absorption of ultraviolet light. Electronic absorption is thought to either promote direct loss of nitrogen to give a carbene or proceed *via* a two-step mechanism in which photoisomerisation to the diazo species, followed by thermal or secondary photochemical release of N<sub>2</sub>(g) gives the carbene. Carbenes are highly energetic and display reactivity preferences that depend on their spin state.<sup>77</sup> Tang and Lijuan demonstrated the dual reactivity nature of diazirine reagents through an extensive series of labelling and mechanistic experiments (Scheme 11).<sup>166</sup>

The dual reactivity of diazirines was elucidated through a comprehensive mechanistic analysis of model functional groups, which dissected the behaviour of these photoreagents into two principal modes. The first mode pertains to the interaction of a diazo intermediate with the protein, which preferentially reacts with polar amino acids by liberating N<sub>2</sub>. Conversely, apolar amino acids predominantly engage with the carbene intermediate, resulting in heterogeneous products typically generated through bond insertion processes. The mechanistic distinction between these two pathways is supported by deconvolution of many elementary steps that were experimentally accessible with the aid of sophisticated photochemical setups. Other examples of the use of diazirine-based photoreagents include direct crosslinkers for biomolecules,<sup>72</sup> binding site identification for antibiotics on proteins<sup>74</sup> solid-state biomolecule cross-linking<sup>167</sup> and mAb radiolabelling.<sup>73</sup>

## Benzophenones

Benzophenone (BP)-based photoreagents were introduced in 1974 when Galardy and co-workers used this class of reagent to map the binding sites of pentagastrin on BSA.<sup>33</sup> Their



**Scheme 11** Diazirines photolysis under UV light by forming either a diazo or a carbene intermediate. The diazo species can convert to the carbene via thermal or photochemical pathways but can also react with nucleophiles on proteins. The carbene species can label protein by C–H or X–H bond insertion pathways and are more reactive toward apolar residues. In this example, BSA was first derivatised with a commercially available diazirine N-hydroxysuccinimide derivative (known as SDA) then photolysed to form a new covalent bond, stapling the protein and rigidifying the structure.<sup>166</sup> These studies highlight the unique capabilities of diazirines in protein labelling, where their versatile reactivity with both polar and apolar residues under UV irradiation provides a valuable approach for creating covalent linkages to a wide range of biomolecules.



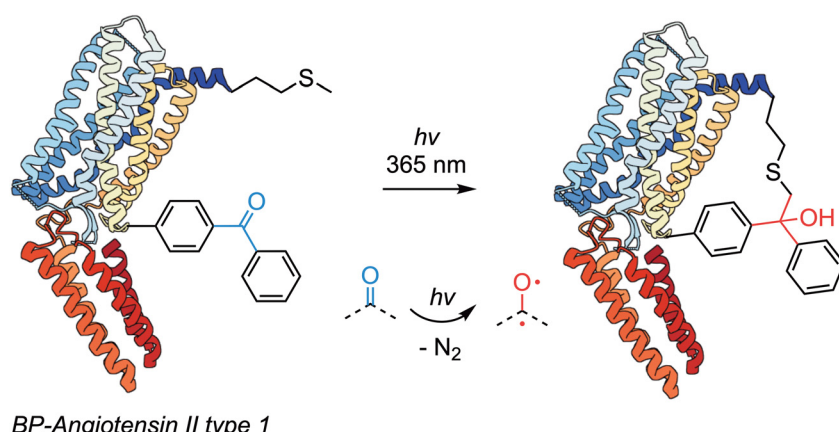
stability, reversible photoactivation in water, and preferential reactivity to otherwise inert C–H bonds (especially methionine residues) crafted the success of this functional group in biomolecule derivatisation.<sup>168</sup> The photoactivation mechanism of BPs involves excitation of the carbonyl chromophore by UV light, which promotes an electron from a non-binding orbital based primarily on the oxygen atom to the antibonding  $\pi^*$  orbital of the carbonyl group. The diradical formed (either as a singlet or triplet species) is very reactive and tends to interact with C–H bonds resulting in hydrogen atom abstraction by the oxygen-centred radical. Ketol radicals and alkyl radicals on the protein then recombine (potentially after intersystem crossing) to form the final products, which results in covalent C–C bond formation between the BP reagent and the biomolecule of interest.

Benzophenone-based compounds have found myriad applications in the radiolabelling of proteins,<sup>169–172</sup> lipids,<sup>173</sup> protein immobilisation<sup>174</sup> and photoconjugation,<sup>175,176</sup> and DNA cross-linking.<sup>177</sup> Of particular interest, is the development of the methionine proximity assay (MPA) – a method for probing protein structure and ligand-receptor interactions which takes advantage of the intrinsic preference of photoexcited BPs for methionine residues located in the vicinity of the photoprobe.<sup>71,178</sup> Seminal work from Escher and colleagues, rigorously investigated a novel Methionine Proximity Assay (MPA) utilising BP photolabelling to elucidate the binding environment of the human angiotensin II type 1 (hAT1) receptor (Scheme 12). By strategically introducing methionine at different positions within transmembrane domains (TMDs) III, VI, and VII, it was possible examine the interaction between these modified sites and photoreactive ligands.<sup>178</sup> Upon photoactivation, BP selectively labels methionine through the formation of a charge-transfer complex. Subsequently, cyanogen bromide (CNBr) cleavage generates distinct fragments, thereby revealing specific ligand-receptor contact points. Overall, BP-based photoreagents are valuable tools in

biochemical research, particularly in elucidating protein–ligand interactions.

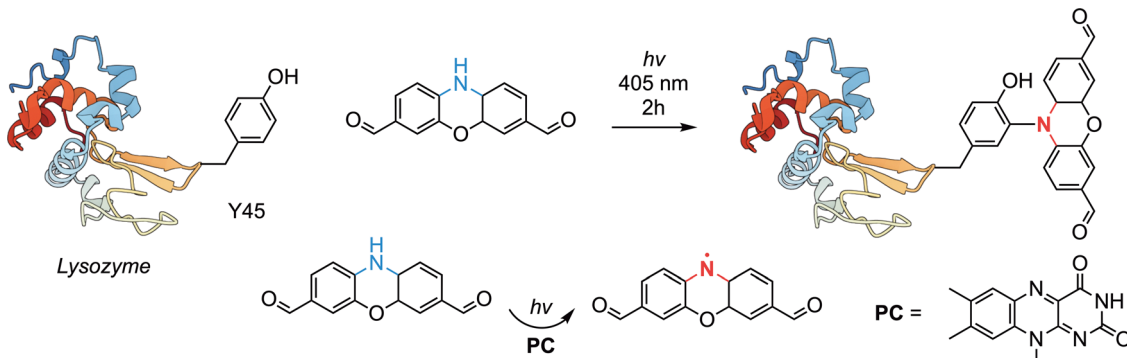
## Photoredox catalysis for bioconjugation

Photocatalysis is a well-established domain in synthetic chemistry,<sup>179</sup> that is also starting to find applications in the functionalisation of biomolecules<sup>180–182</sup> and protein labelling in complex cellular environments.<sup>183</sup> Within this framework, a photosensitive molecule that remains unreactive in its ground state is added to a reaction mixture containing the biomolecule of interest and an inactive substrate. Photoactivation of the catalyst activates a chemical transformation of the substrate, which then reacts with the protein (Scheme 1, mechanism iii). As an example, McMillan and co-workers utilised the redox properties of lumiflavin in its photoexcited state ( $E_{1/2} [{}^3\text{LF}/\text{LF}^{\bullet-}] = 1.68 \text{ V}$ ) to facilitate site-selective *N*-arylation of phenoxazine on the tyrosine residues of lysozyme (Scheme 13). The site-selectivity of the photoredox system is explained by considering solvent exposure of the amino acid substrates on the protein. Lysozyme has three tyrosine residues (Y20, Y45, and Y54) within its primary structure. Two of them (Y20 and Y54) are buried in hydrophobic pockets or engage in cation–π interactions, making them sterically inaccessible or unreactive. On the other hand, Y45 is presented on the protein surface and is solvent-accessible, thus making it a readily available reactive handle. Upon excitation by visible light, the photocatalyst (PC) lumiflavin transforms into the corresponding nitrogen-based triplet diradical, which can abstract a hydrogen atom from phenoxazine, producing the corresponding *N*-radical. The phenoxazine radical then combines with Y45 by expelling a proton and concomitantly reducing lumiflavin to the corresponding dihydro form. The dihydrolumiflavin is then oxidized back to the original lumiflavin by oxygen closing the catalytic cycle. The phenoxazine scaffold allows versatile functional group tolerance. For instance, a phenoxazine dialdehyde was employed as



**Scheme 12** Benzophenones are chromophoric units that undergo reversible photoactivation to give a diradical species in either a singlet or triplet spin state. This diradical can abstract hydrogen atoms from a protein of interest and insert into otherwise unreactive C–H bonds. In this example, BP-derivatised angiotensin II was irradiated with 365 nm light. The electronically excited BP subunit then inserted preferentially into a C–H bond of a proximal methionine residue.<sup>178</sup>





**Scheme 13** Photoredox catalysis proceeds through light-activation of a catalyst which then initiates further chemical transformations on a substrate that can lead to protein bioconjugation. Here, lumiflavin (the photocatalyst, PC) is excited by 405 nm light and undergoes a radical process that abstracts hydrogen from phenoxazine. The phenoxazine radical inserts site-specifically on tyrosine Y45 of lysozyme. By using phenoxazines decorated with additional functional groups (e.g. aldehydes) it is possible to perform further reactions at the heterocycle.<sup>185</sup> Although site-selectivity was reported in this example, for other proteins like mAbs, which present many solvent exposed tyrosine residues, the method is unlikely to be regioselective.

a site-selective reagent for introducing reactive aldehyde groups on protein. Subsequent imination of the aldehydes provided a simple synthetic pathway for introducing additional functional fragments such as fluorophores, affinity tags, terminal alkynes and azides. Notably, the reaction is metal-ion free and operates under mild conditions.<sup>184</sup> Similar strategies that target methionine residues to install functional groups on aprotinin, lactalbumin, myoglobin, human growth hormone, ribonuclease A, and carbonic anhydrase in a site-selective fashion were also reported.<sup>185</sup>

In other examples, the group of Chien-Wei Chiang reported on the use of triphenylpyrylium tetrafluoroborates as photosensitisers for biocompatible photoredox catalysis that facilitates the introduction of pyrazole derivatives on phenylalanine residues under blue light irradiation.<sup>186</sup> Chatterjee and co-workers labelled site-specifically 5-hydroxytryptophan protein derivatives by using methylene blue as the photosensitiser and 455 nm light irradiation.<sup>187</sup> Waser and colleagues reported photoredox catalysed decarboxylative alkynylation to produce peptides with alkynes at the C-terminus. This interesting reaction utilised organic dyes to derivatise peptides in the presence of hypervalent iodine compounds, which acted as the alkynyl transfer reagent.<sup>188</sup> For a comprehensive discussion of metal complex photocatalysed reactions, we direct the reader to recent review by De Jesus *et al.*<sup>189</sup> Collectively, these advancements underscore the versatility and potential of photoredox catalysis to enable chemo- or potentially site-selective modifications on proteins and peptides, though we note that care must be taken to avoid reaction conditions or substrates that might lead to undesired redox reactions (e.g. disulfide reduction) on protein. This growing body of work demonstrates the innovative approaches being developed to leverage visible light in both metal ion complex and organic dye systems, ultimately broadening the tool-kit available for researchers in chemical biology and organic synthesis.

## Conclusions and outlook

This perspective provides a comprehensive overview of the current state of play in the use of photochemical reaction to

functionalise biologically active compounds including proteins and peptides. Reaction characteristics and experimental considerations that must be addressed during optimisation procedures are described with common pitfalls and potential solutions highlighted. Notable examples derived from both historical and contemporary literature on photoinduced bioconjugation chemistry are presented. In most cases, the primary biological substrates used are proteins and polypeptides, while other significant biomolecules have been largely neglected. Consequently, there remains unexplored opportunity for adapting photochemical technologies to functionalise carbohydrates, nucleic acids, and lipids through light-induced reactions. These biomolecules exhibit reactivity patterns that differ markedly from those of proteins and amino acids. Also of particular interest in the future will be the development of bioorthogonal and site-selective photochemical reactions. Considering the broad range of photochemical reactions that remain to be tested in a biological context, and the untapped potential of using new types of covalent bond to construct functional molecules like antibody-drug conjugates for imaging and therapy, we believe that the future looks bright for light-induced biomolecule labelling technologies.

## Author contributions

C. B. wrote the first draft of the manuscript which was revised by J. P. H.

## Data availability

No primary research results, software or code have been included and no new data were generated or analysed as part of this review.

## Conflicts of interest

No potential conflict of interest relevant to this article was reported.



## Acknowledgements

This project has received funding from the European Union's Horizon 2020 research and innovation programme/from the European Research Council (under the Grant Agreement No. 101001734, ERC-CoG-2020, PhotoPHARMA), and from the European Innovation Council Pathfinder grant (grant no. 101129886, SMARTdrugs). JPH also thanks the University of Zurich (UZH) for financial support. We thank all members of the Medicinal Radiochemistry group at the UZH for helpful discussions.

## References

- 1 S. B. Ebrahimi and D. Samanta, *Nat. Commun.*, 2023, **14**, 2411.
- 2 K. Tsuchikama, Y. Anami, S. Y. Y. Ha and C. M. Yamazaki, *Nat. Rev. Clin. Oncol.*, 2024, **21**, 203–223.
- 3 S. B. Ebrahimi and D. Samanta, *Nat. Commun.*, 2023, **14**, 2411.
- 4 A. M. Wu and T. Olafsen, *Cancer J.*, 2008, **14**, 191.
- 5 L. Martiniova, R. J. Zielinski, M. Lin, L. DePalatis and G. C. Ravizzini, *Cancer J. Sudbury Mass.*, 2022, **28**, 446–453.
- 6 G. T. Hermanson and F. L. van Delft, *Chemical Linkers in Antibody-Drug Conjugates (ADCs)*, Royal Society of Chemistry, 2021, pp. 32–70.
- 7 P. Dennler, E. Fischer and R. Schibli, *Antibodies*, 2015, **4**, 197–224.
- 8 R. Fay and J. P. Holland, *J. Nucl. Med.*, 2019, **60**, 587–591.
- 9 J. Li, J. Chen, Q.-L. Hu, Z. Wang and X.-F. Xiong, *Chin. Chem. Lett.*, 2024, 110126.
- 10 B. M. Zeglis, C. B. Davis, D. Abdel-Atti, S. D. Carlin, A. Chen, R. Aggeler, B. J. Agnew and J. S. Lewis, *Bioconjugate Chem.*, 2014, **25**, 2123–2128.
- 11 B. M. Zeglis, C. B. Davis, R. Aggeler, H. C. Kang, A. Chen, B. J. Agnew and J. S. Lewis, *Bioconjugate Chem.*, 2013, **24**, 1057–1067.
- 12 A. Debon, E. Siirola and R. Snajdrova, *JACS Au*, 2023, **3**, 1267–1283.
- 13 E. V. Vinogradova, C. Zhang, A. M. Spokony, B. L. Pentelute and S. L. Buchwald, *Nature*, 2015, **526**, 687–691.
- 14 V. Bacauanu, Z. N. Merz, Z. L. Hua and S. B. Lang, *J. Am. Chem. Soc.*, 2023, **145**, 25842–25849.
- 15 S. R. Thomas, R. Bonsignore, J. Sánchez Escudero, S. M. Meier-Menches, C. M. Brown, M. O. Wolf, G. Barone, L. Y. P. Luk and A. Casini, *ChemBioChem*, 2020, **21**, 3071–3076.
- 16 axispharm, Comprehensive List of FDA-Approved Antibody-Drug Conjugates (ADCs) – Updated for 2024, <https://axispharm.com/antibody-drug-conjugatesadc-list-approved-by-fda2000-2022/>.
- 17 FDA Approved ADC Drugs list up to 2022, <https://www.bio-itworld.com/pressreleases/2022/11/28/fda-approved-adc-drugs-list-up-to-2022>.
- 18 P. Agarwal and C. R. Bertozzi, *Bioconjugate Chem.*, 2015, **26**, 176–192.
- 19 O. Boutureira and G. J. L. Bernardes, *Chem. Rev.*, 2015, **115**, 2174–2195.
- 20 R. Fay and J. P. Holland, *Chem. – Eur. J.*, 2021, **27**, 4893–4897.
- 21 M. Patra, S. Klingler, L. S. Eichenberger and J. P. Holland, *iScience*, 2019, **13**, 416–431.
- 22 A. Guillou, D. F. Earley and J. P. Holland, *Chem. – Eur. J.*, 2020, **26**, 7185–7189.
- 23 D. Lin, L. M. Lechermann, M. P. Huestis, J. Marik and J. B. I. Sap, *Angew. Chem., Int. Ed.*, 2024, **63**, e202317136.
- 24 K. Kozoriz, O. Shkel, K. T. Hong, D. H. Kim, Y. K. Kim and J.-S. Lee, *Acc. Chem. Res.*, 2023, **56**, 25–36.
- 25 L. Wang, Z. Lv, L. Yang, X. Wu, Y. Zhu, L. Liu, Y. Zhao, Z. Huang, D. A. Nicewicz, Z. Wu, Y. Chen and Z. Li, *Bioconjugate Chem.*, 2024, **35**, 1160–1165.
- 26 B. Josephson, C. Fehl, P. G. Isenegger, S. Nadal, T. H. Wright, A. W. J. Poh, B. J. Bower, A. M. Giltrap, L. Chen, C. Batchelor-McAuley, G. Roper, O. Arisa, J. B. I. Sap, A. Kawamura, A. J. Baldwin, S. Mohammed, R. G. Compton, V. Gouverneur and B. G. Davis, *Nature*, 2020, **585**, 530–537.
- 27 P. G. Isenegger, B. Josephson, B. Gaunt, M. J. Davy, V. Gouverneur, A. J. Baldwin and B. G. Davis, *Nat. Protoc.*, 2023, **18**, 1543–1562.
- 28 A. Guillou, D. F. Earley, M. Patra and J. P. Holland, *Nat. Protoc.*, 2020, **15**, 3579–3594.
- 29 A. Singh, E. R. Thornton and F. H. Westheimer, *J. Biol. Chem.*, 1962, **237**, PC3006–PC3008.
- 30 G. W. J. Fleet, R. R. Porter and J. R. Knowles, *Nature*, 1969, **224**, 511–512.
- 31 A. Padwa, S. Nahm and E. Sato, *J. Org. Chem.*, 1978, **43**, 1664–1671.
- 32 A. Padwa, *Acc. Chem. Res.*, 1976, **9**, 371–378.
- 33 R. E. Galardy, L. C. Craig, J. D. Jamieson and M. P. Printz, *J. Biol. Chem.*, 1974, **249**, 3510–3518.
- 34 R. A. G. Smith and J. R. Knowles, *J. Am. Chem. Soc.*, 1973, **95**, 5072–5073.
- 35 R. A. G. Smith and J. R. Knowles, *J. Chem. Soc., Perkin Trans. 2*, 1975, 686–694.
- 36 M. J. Bouchet, A. Rendon, C. G. Wermuth, M. Goeldner and C. Hirth, *J. Med. Chem.*, 1987, **30**, 2222–2227.
- 37 V. Chowdhry, R. Vaughan and F. H. Westheimer, *Proc. Natl. Acad. Sci. U. S. A.*, 1976, **73**, 1406–1408.
- 38 H. Scheefers, C. Schreiber and W. Stoffel, *Hoppe-Seylers Z Physiol. Chem.*, 1978, **359**, 923–931.
- 39 M. P. Goeldner, J. E. Hawkinson and J. E. Casida, *Tetrahedron Lett.*, 1989, **30**, 823–826.
- 40 J. V. Staros and F. M. Richards, *Biochemistry*, 1974, **13**, 2720–2726.
- 41 P. E. Nielsen, J. B. Hansen, T. Thomsen and O. Buchardt, *Experientia*, 1983, **39**, 1063–1072.
- 42 Y. Hatanaka and Y. Sadakane, *Curr. Top. Med. Chem.*, 2002, **2**, 271–288.
- 43 R. B. Woodward, *J. Am. Chem. Soc.*, 1941, **63**, 1123–1126.
- 44 L. F. Fieser, M. Fieser and S. Rajagopalan, *J. Org. Chem.*, 1948, **13**, 800–806.
- 45 T. J. Zbačník, R. E. Holcomb, D. S. Katayama, B. M. Murphy, R. W. Payne, R. C. Cocco, G. J. Evans, J. E. Matsuura, C. S. Henry and M. C. Manning, *J. Pharm. Sci.*, 2017, **106**, 713–733.
- 46 A. L. Daugherty and R. J. Mrsny, *Adv. Drug Delivery Rev.*, 2006, **58**, 686–706.
- 47 D. Schumacher, C. P. R. Hackenberger, H. Leonhardt and J. Helma, *J. Clin. Immunol.*, 2016, **36**, 100–107.
- 48 C. Berton, S. Klingler, S. Prytuliak and J. P. Holland, *npj Imaging*, 2024, **2**, 1–15.
- 49 J. P. Menzel, B. B. Noble, J. P. Blinco and C. Barner-Kowollik, *Nat. Commun.*, 2021, **12**, 1691.
- 50 E. S. Galbavy, K. Ram and C. Anastasio, *J. Photochem. Photobiol., C*, 2010, **209**, 186–192.
- 51 J. Rabani, H. Mamane, D. Pousty and J. R. Bolton, *Photochem. Photobiol.*, 2021, **97**, 873–902.
- 52 K. L. Willett and R. A. Hites, *J. Chem. Educ.*, 2000, **77**, 900.
- 53 F. d'Orchymont and J. P. Holland, *Angew. Chem., Int. Ed.*, 2022, **61**, e202204072.
- 54 S. Klingler and J. P. Holland, *Sci. Rep.*, 2022, **12**, 668.
- 55 P. A. Cieslik, S. Klingler, M. Nolff and J. P. Holland, *Chemistry*, 2024, **30**, e202303805.
- 56 A. Guillou, A. Ouadi and J. P. Holland, *Inorg. Chem. Front.*, 2022, **9**, 3071–3081.
- 57 D. F. Earley, J. Esteban Flores, A. Guillou and J. P. Holland, *Dalton Trans.*, 2022, **51**, 5041–5052.
- 58 B. D. Fairbanks, L. J. Macdougall, S. Mavila, J. Sinha, B. E. Kirkpatrick, K. S. Anseth and C. N. Bowman, *Chem. Rev.*, 2021, **121**, 6915–6990.
- 59 P. Klán, T. Solomek, C. G. Bochet, A. Blanc, R. Givens, M. Rubina, V. Popik, A. Kostikov and J. Wirz, *Chem. Rev.*, 2013, **113**, 119–191.
- 60 A. Poloukhtine and V. V. Popik, *J. Phys. Chem. A*, 2006, **110**, 1749–1757.
- 61 D. A. Sutton and V. V. Popik, *J. Org. Chem.*, 2016, **81**, 8850–8857.
- 62 L. Liu, D. Zhang, M. Johnson and N. K. Devaraj, *Nat. Chem.*, 2022, **14**, 1078–1085.
- 63 Z. Yu, T. Y. Ohulchanskyy, P. An, P. N. Prasad and Q. Lin, *J. Am. Chem. Soc.*, 2013, **135**, 16766–16769.
- 64 J. Deng, X. Wu, G. Guo, X. Zhao and Z. Yu, *Org. Biomol. Chem.*, 2020, **18**, 5602–5607.
- 65 N. K. Devaraj, R. Weissleder and S. A. Hilderbrand, *Bioconjugate Chem.*, 2008, **19**, 2297–2299.
- 66 A. Jemas, Y. Xie, J. E. Pigga, J. L. Caplan, C. W. am Ende and J. M. Fox, *J. Am. Chem. Soc.*, 2022, **144**, 1647–1662.
- 67 A. A. Poloukhtine, N. E. Mbua, M. A. Wolfert, G.-J. Boons and V. V. Popik, *J. Am. Chem. Soc.*, 2009, **131**, 15769–15776.

68 K. Porte, M. Riomet, C. Figliola, D. Audisio and F. Taran, *Chem. Rev.*, 2021, **121**, 6718–6743.

69 H. Maus, A. Gellert, O. R. Englert, J.-X. Chen, T. Schirmeister and F. Barthels, *RSC Med. Chem.*, 2023, **14**, 2365–2379.

70 P. Rousselot, E. Mappus, T. Blachère, M. R. de Ravel, C. Grenot, C. Tonnelle and C. Y. Cuilleron, *Biochemistry*, 1997, **36**, 7860–7868.

71 L. Rihakova, M. Deraët, M. Auger-Messier, J. Pérodin, A. A. Boucard, G. Guillemette, R. Leduc, P. Lavigne and E. Escher, *J. Recept. Signal Transduction*, 2002, **22**, 297–313.

72 A. V. West, G. Muncipinto, H.-Y. Wu, A. C. Huang, M. T. Labenski, L. H. Jones and C. M. Woo, *J. Am. Chem. Soc.*, 2021, **143**, 6691–6700.

73 S. Tamamizu, D. H. Butler, J. A. Lasalde and M. G. McNamee, *Biochemistry*, 1996, **35**, 11773–11781.

74 P. Rotsides, P. J. Lee, N. Webber, K. C. Grasty, J. Beld and P. J. Loll, *ACS Bio Med. Chem. Au.*, 2024, **4**, 86–94.

75 A. Walrant and E. Sachon, *Mass Spectrom. Rev.*, 2024, 1–42.

76 L. Dubinsky, B. P. Krom and M. M. Meijler, *Bioorg. Med. Chem.*, 2012, **20**, 554–570.

77 J. Das, *Chem. Rev.*, 2011, **111**, 4405–4417.

78 P. R. Kym, K. E. Carlson and J. A. Katzenellenbogen, *Bioconjugate Chem.*, 1995, **6**, 115–122.

79 J. Jiang, Y. Liu, S. Yang, H. Peng, J. Liu, Y.-X. Cheng and N. Li, *ACS Med. Chem. Lett.*, 2021, **12**, 1905–1911.

80 Y. Hou, H. Lu, J. Li, Z. Guan, J. Zhang, W. Zhang, C. Yin, L. Sun, Y. Zhang and H. Jiang, *Cell Chem. Biol.*, 2022, **29**, 133–144.e20.

81 E. Karaj, S. H. Sindi and L. M. Viranga Tillekeratne, *Bioorg. Med. Chem.*, 2022, **62**, 116721.

82 S. Chen, C. Liang, H. Li, W. Yu, M. Prothiwa, D. Kopeczynski, S. Loroch, M. Fransen and S. H. L. Verhelst, *ACS Chem. Biol.*, 2023, **18**, 686–692.

83 S. Zhang, P. Liu, L. Li, Z. Liu, X. Qian, X. Jiang, W. Sun, L. Wang and E. U. Akkaya, *ACS Appl. Mater. Interfaces*, 2023, **15**, 40280–40291.

84 Y. Ma, J. Wang, X. Pan, J. Zhang and Y. Shan, *Drug Dev. Res.*, 2023, **84**, 1142–1158.

85 H. Choi, M. Kim, J. Jang and S. Hong, *Angew. Chem., Int. Ed.*, 2020, **59**, 22514–22522.

86 G. S. Kumar and Q. Lin, *Chem. Rev.*, 2021, **121**, 6991–7031.

87 N. P. Gritsan and M. S. Platz, *Chem. Rev.*, 2006, **106**, 3844–3867.

88 C. Bousch, B. Vreulz, K. Kansal, A. El-Husseini and S. Cecioni, *Angew. Chem., Int. Ed.*, 2023, **62**, e202314248.

89 M. D. Holborough-Kerkvliet, G. Mucignato, S. J. Moons, V. Psomiadou, R. S. R. Konada, N. J. Pedowitz, M. R. Pratt, T. Kissel, C. A. M. Koelman, R. T. N. Tjokrodirijo, P. A. van Veenel, T. Huizinga, K. A. J. van Schie, M. Wuhrer, J. J. Kohler, K. M. Bonger, T. J. Boltje and R. E. M. Toes, *Glycobiology*, 2023, **33**, 732–744.

90 Y. Zhang, J. Tan and Y. Chen, *Chem. Commun.*, 2023, **59**, 2413–2420.

91 S. Klingler, R. Fay and J. P. Holland, *J. Nucl. Med.*, 2020, **61**, 1072–1078.

92 D. F. Earley, A. Guillou, S. Klingler, R. Fay, M. Gut, F. d'Orchymont, S. Behmaneshfar, L. Reichert and J. P. Holland, *JACS Au*, 2022, **2**, 646–664.

93 M. J. W. D. Vosjan, L. R. Perk, G. W. M. Visser, M. Budde, P. Jurek, G. E. Kiefer and G. A. M. S. van Dongen, *Nat. Protoc.*, 2010, **5**, 739–743.

94 J. S. Clovis, A. Eckell, R. Huisgen and R. Sustmann, *Chem. Ber.*, 1967, **100**, 60–70.

95 R. Darkow, M. Yoshikawa, T. Kitao, G. Tomaschewski and J. Schellenberg, *J. Polym. Sci., Part A: Polym. Chem.*, 1994, **32**, 1657–1664.

96 H. Meier and H. Heimgartner, *Helv. Chim. Acta*, 1985, **68**, 1283–1300.

97 W. Song, Y. Wang, J. Qu, M. M. Madden and Q. Lin, *Angew. Chem., Int. Ed.*, 2008, **47**, 2832–2835.

98 W. Song, Y. Wang, J. Qu and Q. Lin, *J. Am. Chem. Soc.*, 2008, **130**, 9654–9655.

99 Z. Li, L. Qian, L. Li, J. C. Bernhammer, H. V. Huynh, J.-S. Lee and S. Q. Yao, *Angew. Chem., Int. Ed.*, 2016, **55**, 2002–2006.

100 S. Zhao, J. Dai, M. Hu, C. Liu, R. Meng, X. Liu, C. Wang and T. Luo, *Chem. Commun.*, 2016, **52**, 4702–4705.

101 J. Zhang, J. Liu, X. Li, Y. Ju, Y. Li, G. Zhang and Y. Li, *J. Am. Chem. Soc.*, 2024, **146**, 2122–2131.

102 K. Bach, B. L. H. Beerkens, P. R. A. Zanon and S. M. Hacker, *ACS Cent. Sci.*, 2020, **6**, 546–554.

103 N. L. Kjærsgaard, T. B. Nielsen and K. V. Gothelf, *ChemBioChem*, 2022, **23**, e202200245.

104 W. Feng, L. Li, C. Yang, A. Welle, O. Trapp and P. A. Levkin, *Angew. Chem., Int. Ed.*, 2015, **54**, 8732–8735.

105 S. Jiang, X. Wu, H. Liu, J. Deng, X. Zhang, Z. Yao, Y. Zheng, B. Li and Z. Yu, *ChemPhotoChem*, 2020, **4**, 327–331.

106 J. Zhang, J. Liu, X. Li, Y. Ju, Y. Li, G. Zhang and Y. Li, *J. Am. Chem. Soc.*, 2024, **146**, 2122–2131.

107 Y. Wang, W. J. Hu, W. Song, R. K. V. Lim and Q. Lin, *Org. Lett.*, 2008, **10**, 3725–3728.

108 Z. Yu, L. Y. Ho, Z. Wang and Q. Lin, *Bioorg. Med. Chem. Lett.*, 2011, **21**, 5033–5036.

109 P. An, Z. Yu and Q. Lin, *Org. Lett.*, 2013, **15**, 5496–5499.

110 P. An, Z. Yu and Q. Lin, *Chem. Commun.*, 2013, **49**, 9920–9922.

111 Y. Wang, W. Song, W. J. Hu and Q. Lin, *Angew. Chem., Int. Ed.*, 2009, **48**, 5330–5333.

112 G. Ciamician and P. Silber, *Berichte Dtsch. Chem. Ges.*, 1901, **34**, 2040–2046.

113 F. Sachs and S. Hilpert, *Berichte Dtsch. Chem. Ges.*, 1904, **37**, 3425–3431.

114 B. G. Gowenlock and G. B. Richter-Addo, *Chem. Rev.*, 2004, **104**, 3315–3340.

115 A. Patchornik, B. Amit and R. B. Woodward, *J. Am. Chem. Soc.*, 1970, **92**, 6333–6335.

116 A. Kastrati and C. G. Bochet, *J. Org. Chem.*, 2019, **84**, 7776–7785.

117 C. G. Bochet, *Pure Appl. Chem.*, 2006, **78**, 241–247.

118 T. Šolomek, C. G. Bochet and T. Bally, *Chem. – Eur. J.*, 2014, **20**, 8062–8067.

119 T. Šolomek, S. Mercier, T. Bally and C. G. Bochet, *Photochem. Photobiol. Sci.*, 2012, **11**, 548–555.

120 A. Blanc and C. G. Bochet, *J. Org. Chem.*, 2002, **67**, 5567–5577.

121 C. G. Bochet and A. Blanc, *CRC Handbook of Organic Photochemistry and Photobiology, Two Volume Set*, CRC Press, 3rd edn, 2012.

122 A.-D. Guo, D. Wei, H.-J. Nie, H. Hu, C. Peng, S.-T. Li, K.-N. Yan, B.-S. Zhou, L. Feng, C. Fang, M. Tan, R. Huang and X.-H. Chen, *Nat. Commun.*, 2020, **11**, 5472.

123 A.-D. Guo, D. Wei, H.-J. Nie, H. Hu, C. Peng, S.-T. Li, K.-N. Yan, B.-S. Zhou, L. Feng, C. Fang, M. Tan, R. Huang and X.-H. Chen, *Nat. Commun.*, 2020, **11**, 5472.

124 J. Lai, Y. Xu, X. Mu, X. Wu, C. Li, J. Zheng, C. Wu, J. Chen and Y. Zhao, *Chem. Commun.*, 2011, **47**, 3822–3824.

125 J. M. Tien and I. M. Hunsberger, *J. Am. Chem. Soc.*, 1955, **77**, 6604–6607.

126 S. Kolodych, E. Rasolofonjatovo, M. Chaumontet, M.-C. Nevers, C. Crémion and F. Taran, *Angew. Chem., Int. Ed.*, 2013, **52**, 12056–12060.

127 M. K. Narayananam, Y. Liang, K. N. Houk and J. M. Murphy, *Chem. Sci.*, 2016, **7**, 1257–1261.

128 S. Wallace and J. W. Chin, *Chem. Sci.*, 2014, **5**, 1742–1744.

129 L. Zhang, X. Zhang, Z. Yao, S. Jiang, J. Deng, B. Li and Z. Yu, *J. Am. Chem. Soc.*, 2018, **140**, 7390–7394.

130 V. X. Truong, J. O. Holloway and C. Barner-Kowollik, *Chem. Sci.*, 2022, **13**, 13280–13290.

131 X. Zhang, X. Wu, S. Jiang, J. Gao, Z. Yao, J. Deng, L. Zhang and Z. Yu, *Chem. Commun.*, 2019, **55**, 7187–7190.

132 J. Gao, Q. Xiong, X. Wu, J. Deng, X. Zhang, X. Zhao, P. Deng and Z. Yu, *Commun. Chem.*, 2020, **3**, 1–10.

133 F. P. Woerner, H. Reimlinger and D. R. Arnold, *Angew. Chem., Int. Ed. Engl.*, 1968, **7**, 130–131.

134 E. Albrecht, J. Mattay and S. Steenken, *J. Am. Chem. Soc.*, 1997, **119**, 11605–11610.

135 M.-D. Su, H.-Y. Liao, W.-S. Chung and S.-Y. Chu, *J. Org. Chem.*, 1999, **64**, 6710–6716.

136 R. K. V. Lim and Q. Lin, *Chem. Commun.*, 2010, **46**, 7993–7995.

137 J. O. Mueller, F. G. Schmidt, J. P. Blinco and C. Barner-Kowollik, *Angew. Chem., Int. Ed.*, 2015, **54**, 10284–10288.

138 K. Li, D. Fong, E. Meichsner and A. Adronov, *Chem. – Eur. J.*, 2021, **27**, 5057–5073.

139 N. Z. Fantoni, A. H. El-Sagheer and T. Brown, *Chem. Rev.*, 2021, **121**, 7122–7154.

140 E. Kim and H. Koo, *Chem. Sci.*, 2019, **10**, 7835–7851.



141 C. D. Hein, X.-M. Liu and D. Wang, *Pharm. Res.*, 2008, **25**, 2216–2230.

142 K. Lang and J. W. Chin, *ACS Chem. Biol.*, 2014, **9**, 16–20.

143 N. J. Agard, J. A. Prescher and C. R. Bertozzi, *J. Am. Chem. Soc.*, 2004, **126**, 15046–15047.

144 S. V. Mayer, A. Murnauer, M.-K. von Wrisberg, M.-L. Jokisch and K. Lang, *Angew. Chem., Int. Ed.*, 2019, **58**, 15876–15882.

145 A. Maggi, E. Ruivo, J. Fissers, C. Vangestel, S. Chatterjee, J. Joossens, F. Sobott, S. Staelsens, S. Stroobants, P. V. D. Veken, L. Wyffels and K. Augustyns, *Org. Biomol. Chem.*, 2016, **14**, 7544–7551.

146 T. Läppchen, R. Rossin, T. R. van Mourik, G. Gruntz, F. J. M. Hoeben, R. M. Versteegen, H. M. Janssen, J. Lub and M. S. Robillard, *Nucl. Med. Biol.*, 2017, **55**, 19–26.

147 U. M. Battisti, K. Bratteby, J. T. Jørgensen, L. Hvass, V. Shalgunov, H. Mikula, A. Kjær and M. M. Herth, *J. Med. Chem.*, 2021, **64**, 15297–15312.

148 T. Auchynnikava, A. Äärelä, H. Liljenbäck, J. Järvinen, P. Andriana, L. Kovacs, J. Rautio, J. Rajander, P. Virta, A. Roivainen, X.-G. Li and A. J. Airaksinen, *ACS Omega*, 2023, **8**, 45326–45336.

149 M. Altai, A. Perols, M. Tsourma, B. Mitran, H. Honarvar, M. Robillard, R. Rossin, W. ten Hoeve, M. Lubberink, A. Orlova, A. E. Karlström and V. Tolmachev, *J. Nucl. Med.*, 2016, **57**, 431–436.

150 B. L. Oliveira, Z. Guo and G. J. L. Bernardes, *Chem. Soc. Rev.*, 2017, **46**, 4895–4950.

151 M. M. A. Mitry, F. Greco and H. M. I. Osborn, *Chem. – Eur. J.*, 2023, **29**, e202203942.

152 K. Kang, J. Park and E. Kim, *Proteome Sci.*, 2017, **15**, 15.

153 H. Zhang, W. S. Trout, S. Liu, G. A. Andrade, D. A. Hudson, S. L. Scinto, K. T. Dicker, Y. Li, N. Lazouski, J. Rosenthal, C. Thorpe, X. Jia and J. M. Fox, *J. Am. Chem. Soc.*, 2016, **138**, 5978–5983.

154 J. R. Harbour and S. L. Issler, *J. Am. Chem. Soc.*, 1982, **104**, 903–905.

155 M. Y. Li, C. S. Cline, E. B. Koker, H. H. Carmichael, C. F. Chignell and P. Bilski, *Photochem. Photobiol.*, 2001, **74**, 760–764.

156 V. X. Truong, K. M. Tsang, F. Ercole and J. S. Forsythe, *Chem. Mater.*, 2017, **29**, 3678–3685.

157 T. Posner, *Berichte Dtsch. Chem. Ges.*, 1905, **38**, 646–657.

158 A. K. Sinha and D. Equbal, *Asian J. Org. Chem.*, 2019, **8**, 32–47.

159 Z. Hu, X. Fan, J. Wang, S. Zhao and X. Han, *J. Polym. Res.*, 2010, **17**, 815–820.

160 N. Kotzur, B. Briand, M. Beyermann and V. Hagen, *J. Am. Chem. Soc.*, 2009, **131**, 16927–16931.

161 C. Bao, L. Zhu, Q. Lin and H. Tian, *Adv. Mater.*, 2015, **27**, 1647–1662.

162 M. M. Mahmoodi, S. A. Fisher, R. Y. Tam, P. C. Goff, R. B. Anderson, J. E. Wissinger, D. A. Blank, M. S. Shoichet and M. D. Distefano, *Org. Biomol. Chem.*, 2016, **14**, 8289–8300.

163 E. B. Brown, J. B. Shear, S. R. Adams, R. Y. Tsien and W. W. Webb, *Biophys. J.*, 1999, **76**, 489–499.

164 D. P. Murale, S. C. Hong, Md. M. Haque and J.-S. Lee, *Proteome Sci.*, 2017, **15**, 14.

165 H. Bayley and J. R. Knowles, *Biochemistry*, 1978, **17**, 2420–2423.

166 Y. Jiang, X. Zhang, H. Nie, J. Fan, S. Di, H. Fu, X. Zhang, L. Wang and C. Tang, *Nat. Commun.*, 2024, **15**, 6060.

167 M. D. Congdon and J. C. Gildersleeve, *Bioconjugate Chem.*, 2021, **32**, 133–142.

168 G. Dorman and G. D. Prestwich, *Biochemistry*, 1994, **33**, 5661–5673.

169 J. D. Olszewski, G. Dorman, J. T. Elliott, Y. Hong, D. G. Ahern and G. D. Prestwich, *Bioconjugate Chem.*, 1995, **6**, 395–400.

170 G. Garcia, D. C. Chiara, S. Nirthanan, A. K. Hamouda, D. S. Stewart and J. B. Cohen, *Biochemistry*, 2007, **46**, 10296–10307.

171 D. Yahalom, M. Rosenblatt and M. Chorev, in *Peptides: The Wave of the Future: Proceedings of the Second International and the Seventeenth American Peptide Symposium, June 9–14, 2001, San Diego, California, USA*, ed. M. Lebl and R. A. Houghten, Springer Netherlands, Dordrecht, 2001, pp. 308–309.

172 L.-W. Guo, A. R. Hajipour, M. L. Gavala, M. Arbabian, K. A. Martemyanov, V. Y. Arshavsky and A. E. Ruoho, *Bioconjugate Chem.*, 2005, **16**, 685–693.

173 P. Wang and T. A. Spencer, *J. Labelled Compd. Radiopharm.*, 2005, **48**, 781–788.

174 L. Marcon, M. Wang, Y. Coffinier, F. Le Normand, O. Melnyk, R. Boukherroub and S. Szunerits, *Langmuir*, 2010, **26**, 1075–1080.

175 A. Perols and A. E. Karlström, *Bioconjugate Chem.*, 2014, **25**, 481–488.

176 S. Delaney, Á. Nagy, A. E. Karlström and B. M. Zeglis, *Mol. Imaging Biol.*, 2023, **25**, 1104–1114.

177 J. Jakubovska, D. Tauraité and R. Meškys, *Sci. Rep.*, 2018, **8**, 16484.

178 M. Clément, S. S. Martin, M.-È. Beaulieu, C. Chamberland, P. Lavigne, R. Leduc, G. Guillemette and E. Escher, *J. Biol. Chem.*, 2005, **280**, 27121–27129.

179 M. H. Shaw, J. Twilton and D. W. C. MacMillan, *J. Org. Chem.*, 2016, **81**, 6898–6926.

180 C. Bottecchia and T. Noël, *Chem. – Eur. J.*, 2019, **25**, 26–42.

181 S. J. McCarver, J. X. Qiao, J. Carpenter, R. M. Borzilleri, M. A. Poss, M. D. Eastgate, M. M. Miller and D. W. C. MacMillan, *Angew. Chem., Int. Ed.*, 2017, **56**, 728–732.

182 D. K. Kölmel, J. Meng, M.-H. Tsai, J. Que, R. P. Loach, T. Knauber, J. Wan and M. E. Flanagan, *ACS Comb. Sci.*, 2019, **21**, 588–597.

183 N. E. S. Tay, K. A. Ryu, J. L. Weber, A. K. Olow, D. C. Cabanero, D. R. Reichman, R. C. Oslund, O. O. Fadeyi and T. Rovis, *Nat. Chem.*, 2023, **15**, 101–109.

184 B. X. Li, D. K. Kim, S. Bloom, R. Y.-C. Huang, J. X. Qiao, W. R. Ewing, D. G. Oblinsky, G. D. Scholes and D. W. C. MacMillan, *Nat. Chem.*, 2021, **13**, 902–908.

185 J. Kim, B. X. Li, R. Y.-C. Huang, J. X. Qiao, W. R. Ewing and D. W. C. MacMillan, *J. Am. Chem. Soc.*, 2020, **142**, 21260–21266.

186 Y. Weng, C.-J. Su, H. Jiang and C.-W. Chiang, *Sci. Rep.*, 2022, **12**, 18994.

187 S. J. Singha Roy, C. Loynd, D. Jewel, S. E. Canarelli, E. D. Ficaretta, Q. A. Pham, E. Weerapana and A. Chatterjee, *Angew. Chem., Int. Ed.*, 2023, **62**, e202300961.

188 M. Garreau, F. Le Vaillant and J. Waser, *Angew. Chem., Int. Ed.*, 2019, **58**, 8182–8186.

189 I. S. De Jesus, J. A. C. Vélez, E. F. Pissinati, J. T. M. Correia, D. G. Rivera and M. W. Paixao, *Chem. Rec.*, 2024, **24**, e202300322.

